GEAR TECHNOLOGY

MAY/JUNE 2003

The Journal of Gear Manufacturing

www.geartechnology.com

GEAR CUTTING TOOLS

- Skiving Hobs and Finishing Carburized Gears
- Two-Sided Ground Bevel Gear Cutting Tools

ALSO IN THIS ISSUE

- Retained Austenite & Fatigue Performance
- Worm Scoring & Cracking

THE GEAR INDUSTRY'S INFORMATION SOURCE

GLEASON BRINGS YOU THE LATEST TECHNOLOGY IN PLATED GRINDING WHEELS AND DRESSING TOOLS

Gleason Cutting Tools offers a new line of high-precision replatable CBN and diamond grinding and dressing wheels, for use with any modern CNC gear profile, gear honing or gear grinding machine.

This line of precision tools is available in a wide range of designs, configurations and sizes to meet any special form or gear grinding application.

The use of Gleason single layer CBN technology helps deliver higher stock removal rates, lower cost per workpiece, longer wheel life and more consistent quality. CMM verification of ground coupons is available for the highest quality assurance.

The investment in Gleason Cutting Tools' new state-of-the-art precision plating facility assures the highest quality, consistency and faster deliveries.

For more information, contact:

Gleason Cutting Tools
CORPORATION

ISO 14001 Registered
ISO 9001 Registered

1351 Windsor Road
Loves Park, IL 61111 USA
Website: www.gleason.com

Phone: 815-877-8900
Fax: 815-877-0264
E-Mail: gctc@gleason.com

See us at Gear Expo '03 — Booth #100

GEAR TECHNOLOGY

MAY/JUNE 2003

The Journal of Gear Manufacturing

CUTTING TOOLS ISSUE

34

FEATURES

18

DEPARTMENTS

48

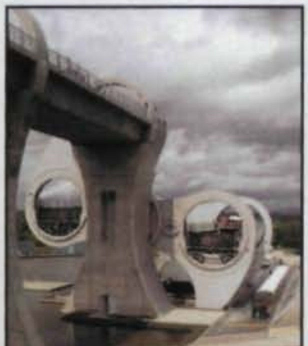

Cover photo courtesy of British Waterways, Scotland.

GEAR TECHNOLOGY

The Journal of Gear Manufacturing

EDITORIAL

Publisher & Editor-in-Chief Michael Goldstein

Managing Editor William R. Stott
Associate Editor Joseph L. Hazelton
Assistant Editor Robin Wright
Editorial Consultant Paul R. Goldstein

Technical Editors
Robert Errichello
Don McVittie
Robert E. Smith
Dan Thurman

ART

Art Director Jean Bartz

ADVERTISING

Advertising Manager Patricia Flam
Advertising Coordinator Carol Tratar

CIRCULATION

Circulation Coordinator Carol Tratar

INTERNET

Web Developer Dan MacKenzie

***Gear Industry Home Page*™ Sales**
Patricia Flam

***powertransmission.com*™ Sales**
Michael A. Gianfrancesco

RANDALL PUBLISHING STAFF

President Michael Goldstein
Vice President Richard Goldstein
Accounting Dianne Borg

Phone: 847-437-6604
E-mail: *people@geartechnology.com*
Web: *www.geartechnology.com*
www.powertransmission.com

BPA INTERNATIONAL

VOL. 20, NO. 3

GEAR TECHNOLOGY, The Journal of Gear Manufacturing (ISSN 0743-6858) is published bimonthly by Randall Publishing, Inc., 1425 Lunt Avenue, P.O. Box 1426, Elk Grove Village, IL 60007, (847) 437-6604. Cover price $5.00 U.S. Periodical postage paid at Arlington Heights, IL, and at additional mailing office (USPS No. 749-290). Randall Publishing makes every effort to ensure that the processes described in GEAR TECHNOLOGY conform to sound engineering practice. Neither the authors nor the publisher can be held responsible for injuries sustained while following the procedures described. Postmaster: Send address changes to GEAR TECHNOLOGY, The Journal of Gear Manufacturing, 1425 Lunt Avenue, P.O. Box 1426, Elk Grove Village, IL, 60007.


• Improve hobbing speed
• Lower costs
• Raise quality
LC 80
LIEBHERR
Liebherr hobbing technology does it all. As the pioneer of high-speed dry machining for gear cutting, Liebherr has compressed cycle times and improved quality with innovative machine features. Our CNC hobbing machines cover the full spectrum of gears up to a diameter of 4500 mm. Over 1,000 installations of this machine concept testify to its acceptance. Couple all this with over 50 years of experience and support, and your choice for gear hobbing has to be Liebherr.
SIGMA POOL
The Gearing Partnership of Liebherr, Klingelnberg and Oerlikon
Liebherr Gear Technology Co.
1465 Woodland Drive
Saline, MI 48176-1259
734.429.7225 • Fax 734.429.2294
info@lgt.liebherr.com
LIEBHERR
Gear Hobbing • Shaping • Grinding • Measuring

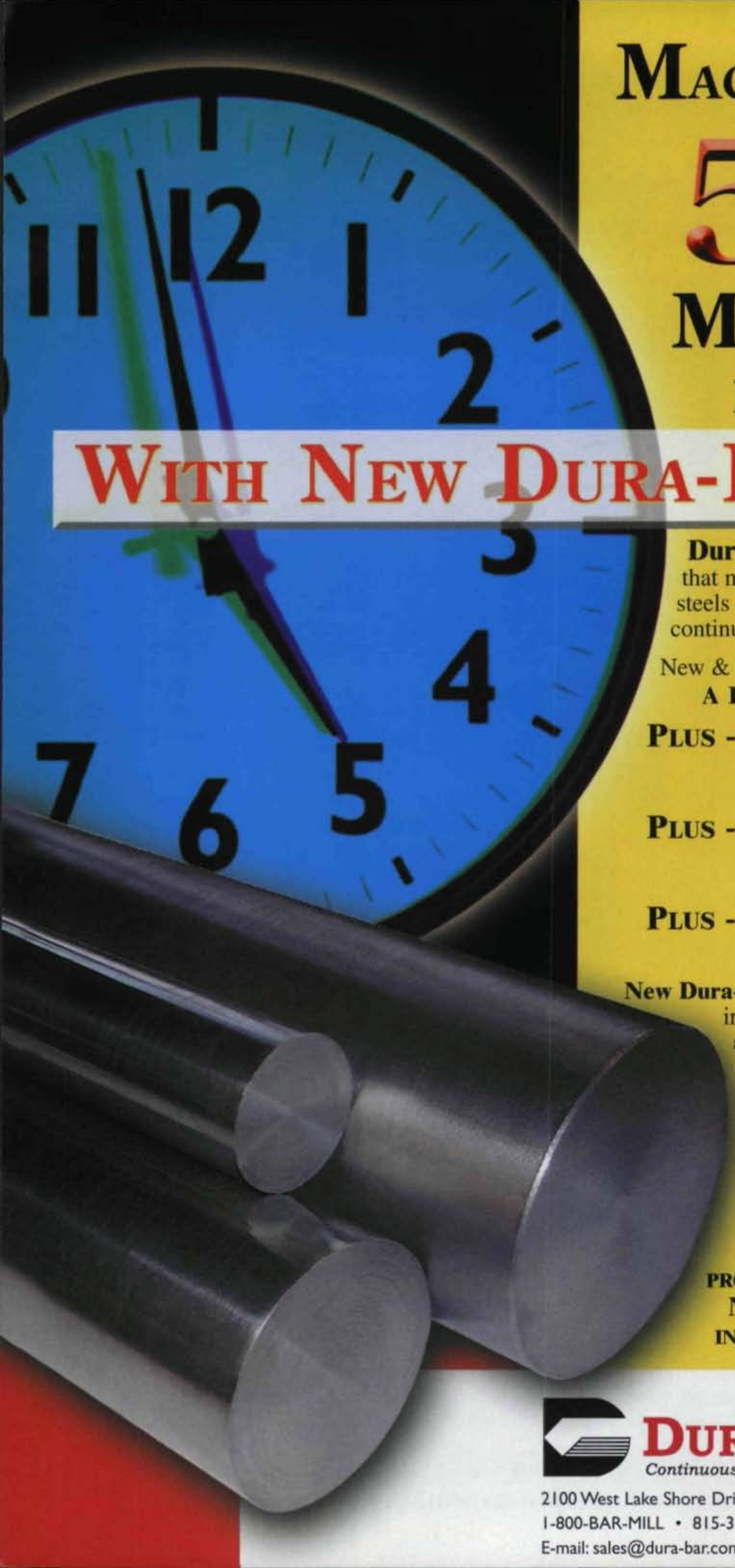

Holding Our Breath

As we sign off on this issue, the war has just begun in Iraq. The world seems to be holding its breath, and waiting.

Prior to the war, it had seemed that the U.S. manufacturing economy had finally bottomed out and was beginning to show signs of activity. But now, the world waits to see how the situation in the Middle East will play out and how the war will affect nations that have been close allies for much of the last century—and longer—but now have very diverse viewpoints on their own best interests.

I had hoped to be able to write about the possibility of an economic upswing, but now I just hope that the pause caused by the uncertainty of war won't sap whatever strength and momentum the economy was accumulating.

I'm still hopeful that manufacturing activity will pick up by the end of summer. If activity does pick up, Gear Expo, October 5–8 in Columbus, OH, could be coming at the perfect time. With any luck, the stars will line up just right: The war will have ended, and everyone will have gotten back to more peaceful pursuits—our lives, our plans and rebuilding our economy.

Gear Expo only comes every two years, and recession or not, the technology doesn't stand still. Even if you're not in the market to buy any technology, Gear Expo is a fast, easy, and inexpensive way to see and learn about current technology. You can talk to the people who design, build, install, service and sell the equipment. You can meet much of the team of most every manufacturer, in one place. Going to the show can only help develop new relationships—and possibly new business—and facilitate the quick gathering of a wide variety of information. Those of you who do your research now will know best what to do when good fortune smiles on you.

All of us at *Gear Technology* will be there, along with a lot of other folks, looking for you to visit us. Stop by our booth to renew your free subscription, and you'll become eligible to win one of our worm/worm wheel clocks. We're also giving away a Grand Prize gear sculpture, as we have at past shows.

So make your hotel reservations now and start looking over the airline schedules. Hopefully, we'll have a good summer and look forward to the fall and Gear Expo with anticipation. At the show, you'll find solutions to increase your productivity and technology, and I'm sure you'll get a warm welcome from everyone there.

Michael Goldstein,
Publisher & Editor-in-Chief

Lifting Boats, Measuring Gears

Giant Geared Wheel Lifts, Lowers Boats in Scotland

In past centuries, the Forth & Clyde and Union canals were an important commercial transport corridor stretching 68 miles across central Scotland.

Boats had to pass through a series of 11 locks to go between the Forth & Clyde Canal and the higher Union Canal.

Today, boats go between the two canals and pass through only three locks. The remaining vertical distance is covered with the help of three large spur gears.

Those gears are part of a huge rotating boatlift at the Forth & Clyde end of the waterway, by the town of Falkirk, Scotland. Called The Falkirk Wheel, the boatlift and its gears appear on *Gear Technology*'s cover.

The Falkirk Wheel is 115 feet high, 115 feet wide and 100 feet long. It consists of two large arms that rotate around a giant axle. Each arm has a gondola that can carry up to four boats at a time. The wheel itself can lift 1.32 million pounds, 660,000 pounds at each end.

One gear is attached to the wheel's taller concrete column, one is attached to one gondola and one is attached to the other gondola. These steel gears are stability gears, and each one has 88 teeth.

Each gear consists of 22 segment plates. When its plates are assembled, each gear has a pitch circle diameter of 31 feet 2 inches and weighs almost 9,300 pounds.

There also are two steel idler gears, one in each arm, between a gondola gear and the column gear. Each idler gear has 21 rollers that mesh with the teeth of its two mated spur gears.

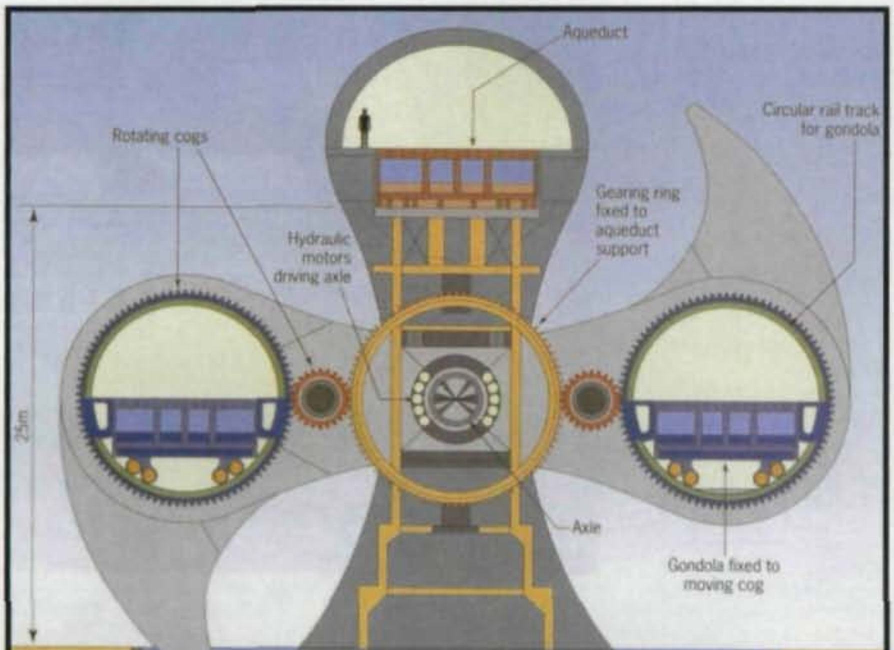

In about five minutes, The Falkirk Wheel raises and lowers boats almost 89 feet via its geared gondolas, passing the boats between aqueduct and basin near Falkirk, Scotland. Five minutes rotates the wheel's arms 180° and is part of the wheel's total transit time of 15 minutes. (The diagram's two small gears became two sets of rollers on the actual wheel.)

***Welcome to* Revolutions*, the column that brings you the latest, most up-to-date and easy-to-read information about the people and technology of the gear industry.* Revolutions *welcomes your submissions. Please send them to* Gear Technology*, P.O. Box 1426, Elk Grove Village, IL 60009, fax (847) 437-6618 or e-mail* people@geartechnology.com. *If you'd like more information about any of the articles that appear, please use* Rapid Reader Response *at* www.geartechnology.com/rrr.htm.**

The wheel's axle is supported by two concrete columns and is driven by 10 hydraulic motors with gearboxes that have 1,000:1 ratios.

Also, the axle is supported on bearings, with an integral 188-tooth ring gear at the drive end. The bearings are each 13 feet in diameter, are located in both concrete columns and can support more than 4 million pounds.

The axle rotates the wheel's two arms. As the wheel rotates, the gondola gears and idler gears rotate around the column gear. The gondolas stay level because they're supported by wheels that run on circular rails in The Falkirk Wheel's arms. The wheels run on sealed, double-row, spherical roller bearings.

The Falkirk Wheel was created as part of The Millennium Link, a major project to reconnect and restore the Forth & Clyde and Union canals.

An important commercial route in the past, the canals were used less and less with the rise of the railroad and later the automobile. In 1963, the British Parliament closed the rights to navigation on the canals. So, the canals weren't maintained to keep them navigable.

"Both canals were built to carry

freight," Robert Jackson says. "They fell into disuse."

Jackson is a mechanical engineer for British Waterways Scotland. British Waterways runs the United Kingdom's canals. British Waterways Scotland is a part of that agency.

The canals' disuse ended in 1998, with the start of The Millennium Link. The canals were made navigable again and were reconnected by The Falkirk Wheel, which became operational in June 2002.

With the canal's rebirth came a new use: leisure. Cruise boats, canoes and luxury boats for hire now ply the waterway.

"It's used commercially for people, but not for hauling goods," Jackson says.

Now the wheel and canals are promoting commercial development along their course. The development includes offices, shops, pubs and restaurants.

That course is new, though. With navigation rights closed and with the automobile's rise, the canals became blocked in more than 30 places by roads built in the 1960s.

To reconnect the two canals, British Waterways extended the Union Canal almost a mile westward, lowered it through two locks, then took it underground—below the main Edinburgh-Glasgow railroad and the historic Antonine Wall, a defensive structure built by the Roman Empire.

The canal then emerges from its 480-foot tunnel as a 99-foot-high aqueduct. The aqueduct ends at the top of The Falkirk Wheel.

Floating in the wheel's top gondola, boats slowly swing down almost 89 feet to New Port Downie, the wheel's boat basin. Boats then pass through a lock and are down in the Forth & Clyde Canal.

Crowning this engineering feat is acknowledgment of The Falkirk Wheel as a machine that achieves the level of art.

The Royal Fine Art Commission for Scotland says The Falkirk Wheel was "a definite attempt to design the wheel for the 21st century. This design is considered to be a form of contemporary sculpture . . . a truly exciting solution."

Analyze Gears Without Locking Out Measurement Values

The ND430 Next Dimension® measuring analysis system from Process Equipment Co. of Tipp City, OH, is designed to measure post-heat treatment distortion or injection molding shrinkage.

The measuring software develops a

link between tooth thickness and helix/involute measurements. With standard analysis methods, form deviations are visible. With the Process Equipment analysis, traces are plotted to their absolute position in space relative to a design tooth thickness.

This allows designers to see the position along the face width and involute where every measured tooth will be oversized or undersized. With plastic and powder metal gears, this data can be used to more quickly adjust manufacturing parameters for making acceptable parts. Also, if tooth thickness varies around a gear's circumference, designers can see the effects on helix and involute forms.

"If you're only performing conventional helix and involute measurements (not tooth size), the effects from machine volumetric accuracy are of lesser importance, except when you are measuring a gear that is at a diameter or height different than the calibration artifact for that machine" says Mark Cowan, director of metrology for Process Equipment.

"However, when you are determining tooth size, absolute probe positioning in space becomes very important. With our package, we have verified the accurate probe positioning in space for the entire machine measuring volume by mapping the full travel of each of the x-, y- and z-axes. This is unique in the industry."

Normally a measuring probe moves when it contacts the tooth surface. Most systems "lock out" these measurement values.

These measurements, combined with their volumetric mapping, ensure the machine knows the probe's location in space, allowing it to accurately measure tooth thickness.

Data can be shared with process equipment and finishing tool manufacturers because the program creates files of the average compared helix and involute traces.

Similar systems are made by other companies, such as Klingelnberg Co. of Saline, MI, and M&M Precision Systems Corp. of West Carollton, OH.

Federal Mogul's sintered processes division bought a less sophisticated version of the Process Equipment system in 2001 to inspect process changes. They chose Process Equipment, partly because of its measurement certainty of 0.002 mm or 2 microns, with some micron repeatability.

"The main reason Federal Mogul bought the ND430 is because it was able to inspect an unknown root area using a 3-D probe," says Jason Barnhart, process development engineer at Federal Mogul.

Tell Us What You Think . . .
Visit *www.geartechnology.com* to
- **Rate this column**
- **Request more information**
- **Contact the companies mentioned**
- **Make a suggestion**

Or call (847) 437-6604 to talk to one of our editors!

Characterization of Retained Austenite in Case Carburized Gears and Its Influence on Fatigue Performance

Fouad B. Abudaia, J. Terry Evans and Brian A. Shaw

Carburized helical gears with high retained austenite were tested for surface contact fatigue. The retained austenite before testing was 60% and was associated with low hardness near the case's surface. However, the tested gears showed good pitting resistance, with fatigue strength greater than 1,380 MPa.

Detailed examination carried out on a gear that had been tested by contact on one flank on each tooth in a back-to-back test revealed that about 50% of the initial retained austenite was transformed to martensite during the test. Transformation was stress- or strain-assisted and was limited to a thin layer of 10 µm thickness or less at the surface. The increase in surface contact fatigue strength is attributed to the increased compressive residual stress and hardness in the mechanically transformed layer.

Introduction

High performance gears are case hardened to increase the hardness of the surface layer and thereby impart resistance to surface contact fatigue.

Table 1—Chemical composition of the investigated steel (percentage by weight).	
C	0.17
Si	0.27
Mn	0.5
P	0.008
S	0.0039
Cr	1.66
Mo	0.28
Ni	1.5
Cu	0.15
Sn	0.011
Al	0.023
N	0.007
V	0.004

Table 2—Helical test gear dimensions.

Gear Property	Value
Helix angle (degrees)	30
Number of teeth	23
Module (mm)	6.0
Gear ratio	1:1
Center distance (mm)	160
DIN quality	5
Face width (mm)	38
Base circle diameter (mm)	150.35
Addendum (mm)	6.0
Tip diameter (mm)	172.0
Root diameter (mm)	142.7
Base pitch error (µm)	7.0
Form error (µm)	8.5
Tip relief (µm/mm)	70 µm over 0.8 mm
Total error (µm)	9.5

Case carburizing is extensively used for this purpose in gears and bearings. Carburization of the case increases the carbon content to levels between 0.8% and 1%. Also, subsequent heat treatment is used to produce a tempered martensitic structure with some retained austenite.

A number of standard heat treatments in gear applications require the retained austenite to be in the range of 15–20%. On the other hand, in aerospace applications, other standards require the retained austenite to be reduced to less than 4% by sub-zero cooling.

Generally, the effect of retained austenite on fatigue is not entirely clear. Zaccone et al. (1989) showed that high levels of retained austenite increased fatigue strength in bending fatigue in the low- to medium-cycle regime but reduced fatigue strength in the high-cycle regime.

One explanation is: Retained austenite, being softer than tempered martensite, imparts a high level of fracture toughness, which is beneficial in the low-cycle fatigue regime, where much of the fracture life is taken up with Stage II crack growth. Relatively little information has been published on the effect of retained austenite on the surface contact fatigue performance of gears.

In this paper, we present the results of back-to-back tests on case carburized gears with high retained austenite contents. Despite the fact that the hardness of the material in the case was significantly lower than in gears with normal retained austenite contents, the pitting fatigue resistance of the high austenite gears is good. It is believed that stress-induced transformation of retained austenite to martensite in a thin layer close to the surface is responsible for the relatively good pitting fatigue resistance.

Method and Materials

The performance of helical test gears made from low alloy steel containing a high level of retained austenite in the carburized case was investigated. The chemical composition of the gear material prior to case carburization is given in Table 1. The dimensions of the gear are given in Table 2.

The contact fatigue SN curve for these gears was determined by testing in a recirculating power, back-to-back test rig. Gears are considered failed when 4% of the involute flank areas contain pits or when obvious fracture took place. The SN curve is compared with that of low alloy steel containing a normal amount of retained austenite as shown in Figure 1.

The loaded flank was run for 32 million cycles with a contact stress of 1,455 MPa. The contact stress is the maximum stress operating in the area of contact between the involute flanks.

After the fatigue tests were conducted, a gear, which was run by contact of one flank of each tooth, was selected for examination. Teeth from the selected gear were removed, and tests were carried out on both the run and the un-run flanks.

Microhardness profiles on tooth cross sections were carried out with a 300 g load. The first indentation was taken at a distance of 50 µm from the surface. Retained austenite was measured by X-ray diffraction with a K_α radiation beam using AST-Stresstech's Xstress 3000 residual stress analyzer. Profiles up to a depth of 50 µm were made on both flank sides.

The Xstress 3000 residual stress analyzer was also used for residual stress measurements. Measurements were made on two orthogonal directions, the longitudinal direction or grinding direction and the direction transverse to the grinding direction. Note that the gears are ground in a direction parallel to the axis of the gear. The direction parallel to the grinding direction will be referred to as the 0° direction and the direction normal to this as the 90° direction. Profiles of the residual stresses in the martensite and the austenite phases were obtained to a depth of 50 µm.

Vickers macrohardness was used to measure the hardness of the run and un-run surfaces. One tooth was cut into two parts. Both parts were tested in the same manner, except that one part was tested after the removal of a 10 µm layer by etching. Loads of 1 kg, 2.5 kg, 5 kg and 10 kg were used on each side. The penetration depth of the indentor decreases as the testing loads decrease. Under smaller loads, the test could be confined to layers near to the surface. In addition, microhardness profiles were obtained in metallographic sections of the gear teeth.

In order to obtain more evidence for the changes that took place at and near the surface, optical microscopy examination was carried out on a metallographic section of a cut tooth.

Results

The retained austenite and the microhardness profile for the un-run flank are shown in Figures 2 and 3, respectively. These figures show the high level of the retained austenite associated with the low hardness values at a depth down to 0.8 mm below the surface.

Figure 4 shows the retained austenite profile in the run flank side. The level of the retained austenite was substantially decreased at the surface and near the surface compared with the un-run flank. The change from 60% in the un-run flank to 34% in the run flank was limited to a shallow depth.

Figures 5a and 5b show the surface macrohardness measurements versus depth of indentation for the un-etched and the etched parts of the tested tooth, respectively. The depth of indentation was varied by changing the applied load between 1 and 10 kg. The hardness of the run and un-run flanks was clear-

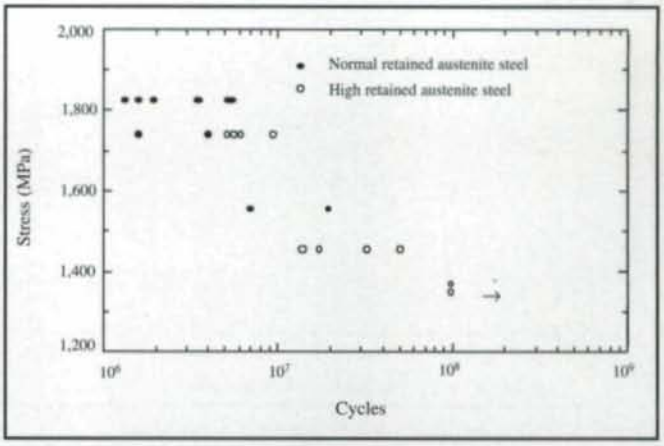

Figure 1—Stress vs. number of cycles for pitting fatigue in helical test gears. (The arrow indicates run out.)

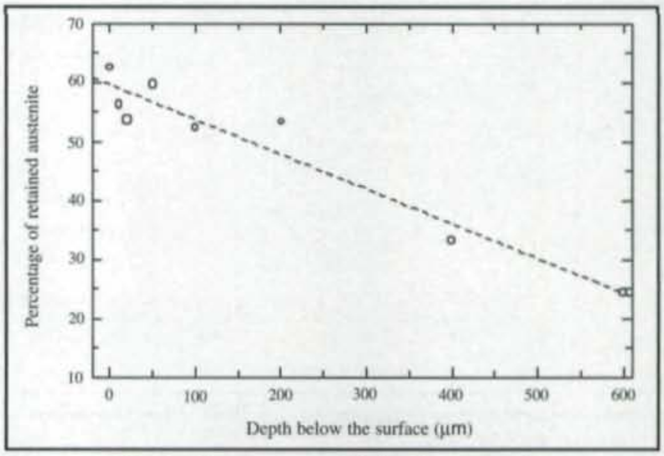

Figure 2—Retained austenite profile in the un-run flank.

Fouad B. Abudaia

is a doctoral student in the mechanical and systems engineering school at the University of Newcastle upon Tyne, United Kingdom. He holds a master's degree in material science and is performing research on the microstructure and fatigue strength of high performance gear steels.

J. Terry Evans

is a professor of materials engineering and acting head of the mechanical and systems engineering school in the University of Newcastle upon Tyne. He holds a doctorate in metallurgy and has published more than 200 papers in the field of deformation, fatigue and fracture of materials.

Brian A. Shaw

is a senior materials engineer with Design Unit, a part the mechanical and systems engineering school at University of Newcastle upon Tyne. A self-funded agency, Design Unit serves industry through research and consultancy, mainly in the field of gearing and mechanical power transmissions. Shaw holds a doctorate in materials engineering and has experience in metallurgical characterization of gear materials and fatigue failures. Also, he has consulted in areas related to residual stress, fatigue performance and material quality control in gear steels.

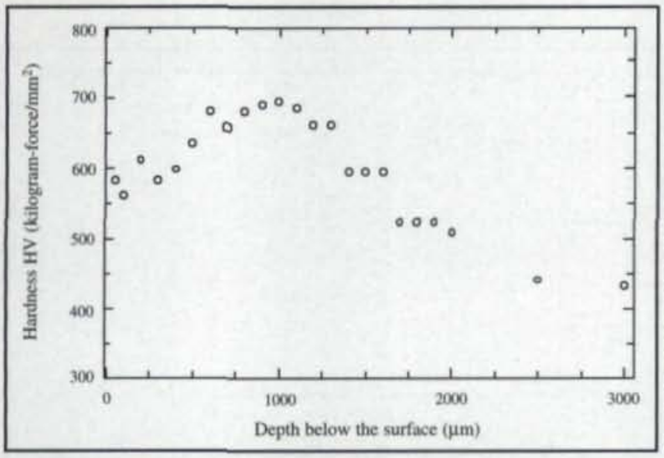

Figure 3—Microhardness profile for the un-run flank.

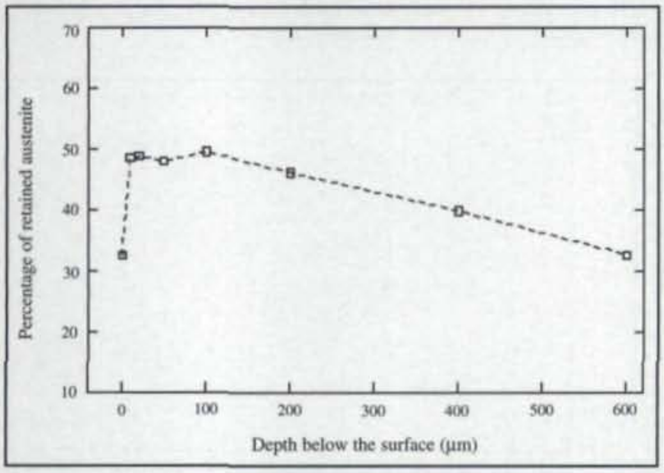

Figure 4—Retained austenite in the run flank after 32 million cycles at a surface contact stress of 1,455 MPa.

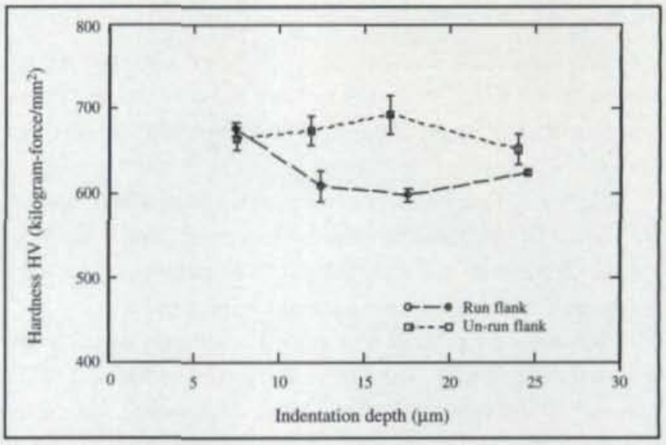

Figure 5a—Surface hardness as a function of indentation depth, before surface layer removal.

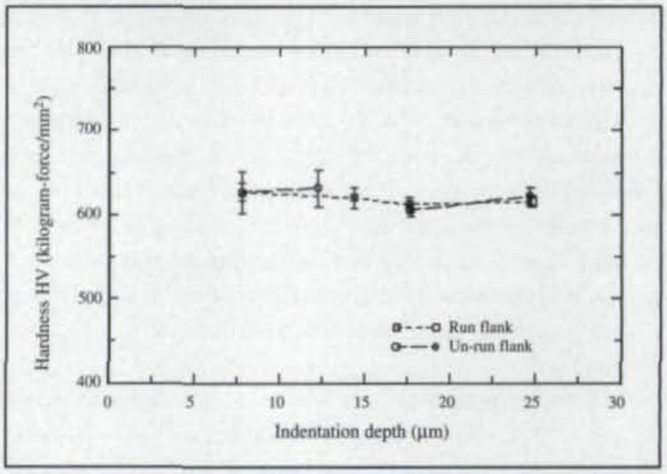

Figure 5b—Surface hardness as a function of indentation depth, showing the effect of surface layer removal.

ly different for the un-etched specimen (Fig. 5a). However, after etching 10 μm, the hardness values of the run and un-run flanks were sensibly the same (Fig. 5b).

Changes at shallow depths were also noticed for residual stress measurements. Residual stress profiles were measured in the run and un-run flanks in both the martensite and the retained austenite. In addition, residual stresses were measured in the 0° and 90° directions. The results are shown in Figures 6a–6d.

Figures 6a and 6b compare the residual stress profiles in the martensite phase for the run and un-run flanks on the 0° and the 90° directions, respectively.

Residual stresses in the austenite phase on both flanks and directions are shown in Figures 6c and 6d.

In the martensite phase in the 0° direction, the run flank showed a large compressive stress at the surface, whereas the un-run flank exhibited only a small compressive stress. In the martensite in the 90° direction, the un-run flank showed a residual stress of just less than –400 MPa while the run flank showed a stress just greater than –500 MPa. At depths greater than 10 μm, there was little difference between the run and un-run flanks.

A greater difference in the residual stress distributions down to a greater depth was observed in the austenitie phase in the 0° direction (Fig. 6c). However, a smaller difference was observed in the 90° direction (Fig. 6d).

Microstructures near the run and un-run sides of the same tooth are shown in Figures 7a and 7b, respectively. The microstructure was typical of material with large austenite grain size. Plates of martensite were clearly visible within the austenite matrix. A higher martensite plate content was evident near the surface of the run flank. This supports the idea that stress-assisted or strain-assisted martensite transformation occurred during surface contact.

Discussion

The high retained austenite content in the case of the carburized gear teeth produces a relatively low hardness down to a depth of 0.5 mm (Figs. 2 and 3). Despite the substandard hardness level, the gears with high retained austenite have good pitting fatigue resistance, with strength greater than 1,380 MPa at 10^8 cycles. Certainly, if fully martensitic specimens were over-tempered to produce a similar low hardness, one would expect to see a significantly reduced pitting fatigue strength.

The evidence from hardness tests, X-ray diffraction and metallographic examination suggests that the good fatigue resistance is due to either stress- or strain-induced martensite transformation in a thin layer near the surface of the run involute flanks.

Figure 6—Residual stress distribution in the martensite and austenite phases.

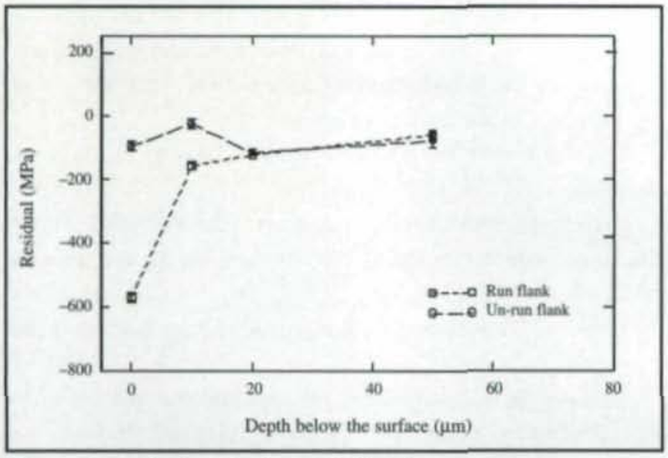

Figure 6A—Martensite phase, 0° direction

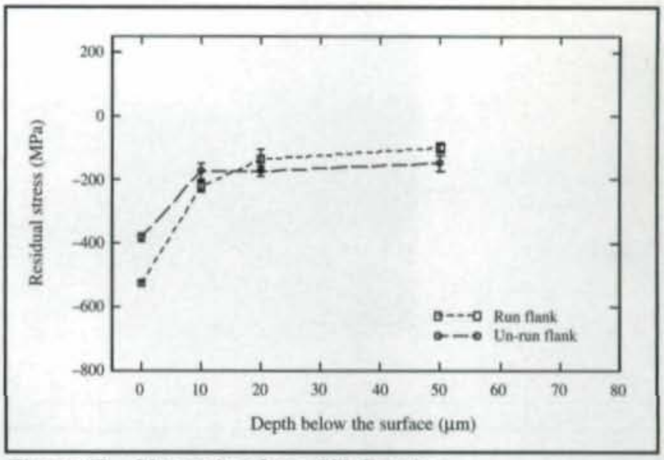

Figure 6B—Martensite phase, 90° direction

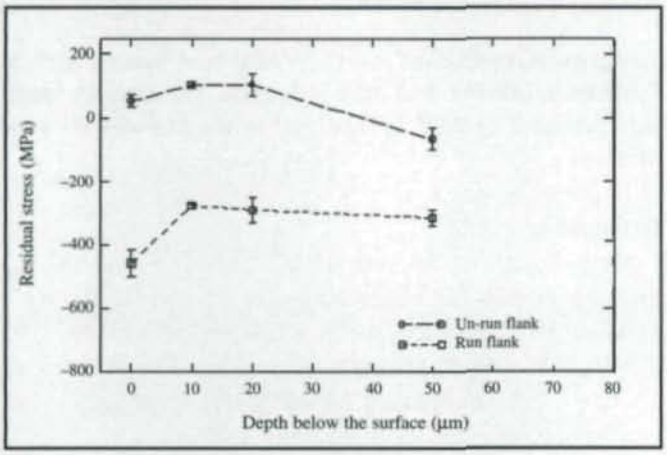

Figure 6C— Austenite phase, 0° direction

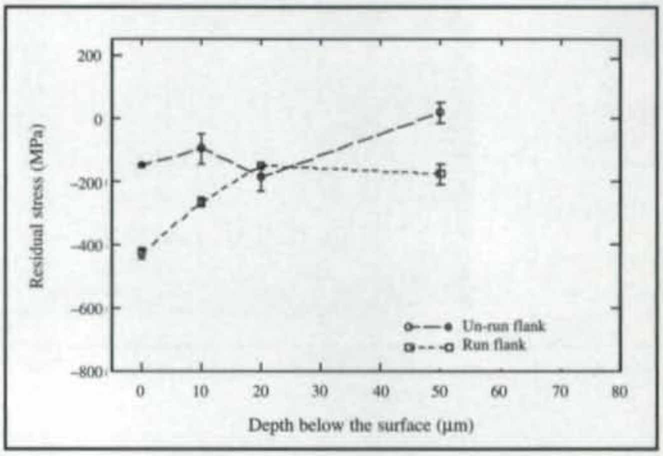

Figure 6D—Austenite phase, 90° direction

There is clear evidence that surface contact in the back-to-back tests reduces the retained austenite content at the surface by a factor of two. In the un-run flanks, the retained austenite content is of the order of 55–63% (Fig. 2). After cycling surface contact in the back-to-back tests, the retained austenite content at the surface was found to be reduced to the level of 30–35% (Fig 4).

The thin layer of contact-reduced retained austenite is of the order of 10 μm. This conclusion is supported by the surface hardness results in Figures 5a and 5b. In Figure 5a, the un-run surface shows a lower hardness than the run flank at penetration depths between 12 and 18 microns. Also in Figure 5a, at greater penetration depths, the hardness values converge. At the smallest penetration depth of 7 μm, the hardness values for the run and un-run flanks again converge. It is believed that, at the small indentor depth, the influence of strain hardening from grinding during manufacture is dominant, i.e. both run and un-run involute flanks were ground in the final stage of manufacture.

After the 10 μm surface layer was removed by etching, the hardnesses of run and un-run flanks were sensibly identical at all indentor penetration depths in the range 7–25 μm (Fig. 5b). This latter evidence supports the idea that significant hardness increases occur as a result of surface contact, but only to a depth of 10 μm or less. We note, however, that the relation between hardness and depth of indentation (Fig. 5a) does not give a direct relation between the measured hardness and the hardness gradient in the material surface layers, because the harder layer near the surface continues to influence measured hardness at penetration depths greater than the hardness of the layer.

The mechanism of stress- or strain-induced austenite to martensite transformation at the gear surface remains to be understood in detail. It is known that the transformation of retained austenite can be nucleated by externally imposed stress (or elastic strain) acting alone and by plastic strain (Olson, 1982). Maxwell et al. (1974) reported a different morphology for martensite produced by the aid of stress and plastic strain. In addition, stress-assisted and plastic-strain-assisted martensite formation operates over different temperature ranges. Stress-assisted martensite transformation occurs predominantly below a characteristic temperature M_s^σ while plastic-strain-assisted martensite occurs between M_s^σ and a higher temperature M_d. At temperatures above M_d, neither stress-assisted nor strain-assisted transformation of retained austenite occurs. Neu and Sehitoglu (1991) found for carburized 4320 steel that stress-induced transformation occurred between 22°C and 60°C.

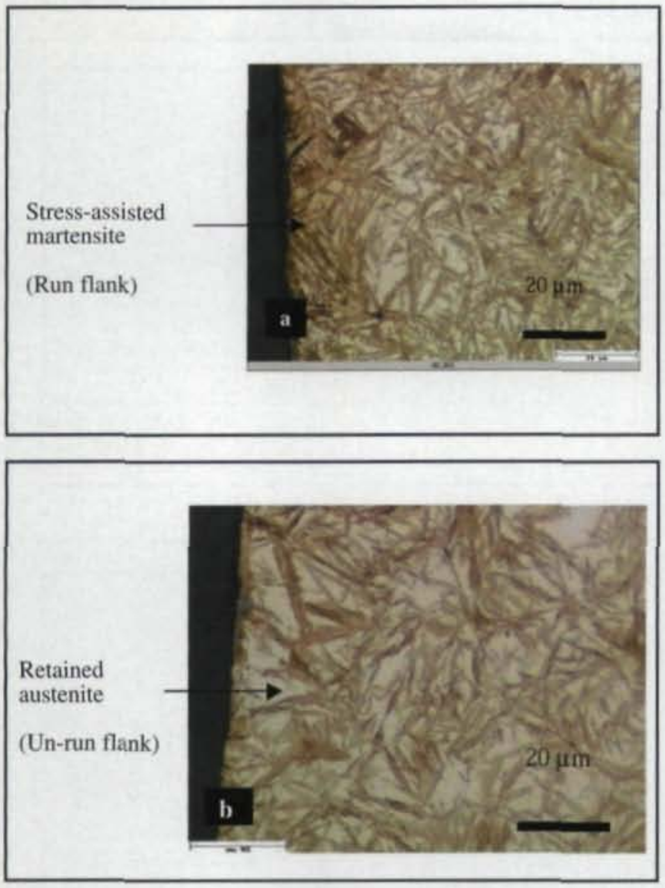

Figure 7—Microstructures in the run and un-run flanks.

A further observation is that compressive axial stress or hydrostatic stress suppresses the transformation, while axial or hydrostatic tension favors it. Thus, little strain-assisted transformation is observed when the plastic deformation occurs with a superimposed hydrostatic pressure, while the greatest amount of transformation occurred under axial tension (Neu and Sehitoglu, 1992). These observations are pertinent to the present results because the stress field produced by surface contact of the involute flanks is predominantly compressive.

The Von Mises stresses are less than the yield strength of the material for ideally smooth surfaces. Thus, any plastic deformation in the involute flanks must occur at the scale of the surface asperities. Even so, the superimposed hydrostatic stress is predominantly compressive, thereby acting to oppose strain-induced martensite transformation.

Surface contact had an effect on residual stresses only near the surface. As shown in Figure 6a, surface contact produced a significant surface residual compressive stress in the 0° direction. This is consistent with stress- or strain-induced martensite transformation, which is expected to produce residual compressive stress because of the associated 4% volume increase. On the other hand, it is believed that the surface residual stress is complicated by the treatment prior to testing. The last operation is surface grinding, and the different residual stresses in the 0° and the 90° directions in the un-run flanks (Figs. 6a and 6b) are typical of near-surface residual stresses produced by a grinding operation.

Conclusions

Gear materials made from steels with high levels of retained austenite showed high fatigue resistance and good performance.

Stress-assisted martensitic transformation occurred under the influence of the contact stresses.

Transformation was confined to a thin layer of about 10 (m in depth.

High compressive stresses are set up in the transformed layer due to constraint imposed by the austenite matrix and the core material.

Martensitic transformation caused the surface hardness to be increased.

Changes in microstructure, residual stresses and hardness were confined to a thin layer of about 10 µm in depth. These are beneficial changes from the surface fatigue point of view and resulted in improved performance. ○

This paper was presented at the 20th ASM Heat Treating Society Conference, held Oct. 9–12, 2000, in St. Louis, MO. Also, the paper was published by ASM International in the conference's proceedings.

References

1. Maxwell, P.C., A. Goldberg and J.C. Shyne. "Stress-Assisted and Strain-Induced Martensite in Fe-Ni-C Alloys," *Metallurgical Transaction*, Vol. 5, 1974, pp. 1305–1318.

2. Neu, R.W. and H. Sehitoglu. "Transformation of Retained Austenite in Carburized 4320 Steel," *Metallurgical Transaction*, Vol. 22A, 1991, pp. 1491–1500.

3. Neu, R.W. and H. Sehitoglu. "Stress-Induced Transformation in a Carburized Steel—Experiments and Analysis," *Acta Metallurgica Et Materialia*, Vol. 40, No. 9, pp. 2257–2268, 1992.

4. Olson, G.B. and M. Cohen. "A Mechanism for the Strain-Induced Nucleation of Martensitic Transformation," *Journal of Less Common Metals*, Vol. 28, pp.107–118, 1972.

5. Zaccone, M.A., J.B. Kelley and G. Krauss. "Strain Hardening and Fatigue of Simulated Case Microstructure in Carburized Steel," *Carburizing: Processing and Performance, ASM International*, Lakewood, Colorado, July 12–14, 1989.

TECHNICAL CALENDAR

May 20–22—Fundamentals of Parallel Axis Gear Manufacturing. Pheasant Run Resort, St. Charles, IL. This seminar, with a limited class size of 35, focuses on gear nomenclature, automation systems, basic gear mathematics, hobbing, skiving, fixturing and blanks, as well as other topics. $750, including meals. For more information, contact Koepfer America L.L.C. at (847) 931-4121 or on the Internet at *www.koepferamerica.com.*

June 8–12—2003 International Conference on Powder Metallurgy & Particulate Materials. Mandalay Bay Resort & Casino, Las Vegas, NV. PM^{2}TEC2003 will offer an extensive technical program that includes seminars for delegates in the powder metallurgy, powder injection molding and particulate materials industries. Costs range from $40–$1,175, depending on the package selected. For more information, contact the Metal Powder Industries Federation by telephone at (609) 452-7700 or by e-mail at *info@mpif.org.*

June 9–12—Basic Gear Fundamentals. Gleason Corp., Loves Park, IL. This four-day program consists of lectures given by engineering, production and inspection staff members to provide an understanding of gear geometry, nomenclature, manufacturing and inspection to people new to the field. Attendees are taken on a tour of Gleason's facility and given demonstrations. Contents of the seminars include gear history, types and ratios, involute gear geometry, gear tooth systems and gear cutting methods. $895 includes a handbook, class materials, lunches and one group dinner. For more information, contact Gleason by telephone at (815) 877-8900 or on the Internet at *www.gleason.com.*

June 9–13—AGMA 2003 Basic Course. Daley College, Chicago, IL. Offers classroom and hands-on training in gearing and nomenclature, principles of inspection, gear manufacturing methods, and hobbing and shaping. $650 for AGMA members, $775 for non-members. For more information, contact AGMA by telephone at (703) 684-0211 or by e-mail at *fentress@agma.org.*

June 23–25—AGMA's Regional Gear Manufacturing Technology Course. Star-SU, Hoffman Estates, IL. $750 per attendee. Three-day course presented by the Gear Consulting Group LLC. For more information, call (866) 202-1699 or send a message to *gearconsulting@aol.com.*

Tell Us What You Think . . .
Visit *www.geartechnology.com* to
- **Rate this column**
- **Request more information**
- **Contact the organizations mentioned**
- **Make a suggestion**

Or call (847) 437-6604 to talk to one of our editors!

Large Scores and Radial Cracks on Case-Hardened Worms

Wolfgang Predki, Friedrich Jarchow, Ralf Dinter and Alexander Rhode

Abstract

In the last couple of years, many research projects dealt with the determination of load limits of cylindrical worm gears. These projects primarily focused on the load capacity of the worm wheel, whereas the worm was neglected. This contribution presents investigations regarding damages such as large scores and cracks on the flanks of case-hardened worms.

Introduction

The load-carrying capacity of cylindrical worm gears is generally limited by the worm wheel made of bronze. This material has a lower strength than the worm made of steel. Critical loads are reached if pitting, sliding wear, tooth breakage, scuffing or high oil temperatures occur. However, in the last couple of years, defects such as radial cracks or large scores have increased on the case-hardened worm surface. These defects can cause an increased wear on the worm wheel, which can lead to a premature loss of drive. This report shows a way to determine the maximum permissible load that leads to these defects, as well as testing new methods which increase the load carrying capacity.

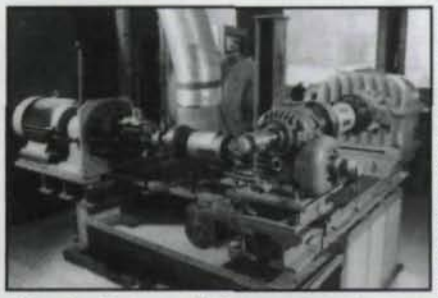

Fig. 1—Test stand for scoring damage, center distance a = 100 mm.

Fig. 2—Test stand for cracking damage, center distance a = 250 mm.

Fig. 3—Large score marks on a case-hardened worm.

Test Conditions

The test runs to examine score marks and cracks on hardened worm flanks were executed separately on two electrically strutted test stands. The mating materials are case-hardened worms made of 16MnCr5 steel and worm wheels made of GZ-CuSn12Ni bronze. Tests for scoring were executed with gear sets with a center distance of a = 100 mm, a gear ratio of i = 41:2, a worm shaft arranged below the worm gear and splash lubrication. Figure 1 shows the test stand that was employed for scoring tests.

After assembly and adjustment of the contact pattern, the worm gear sets were loaded immediately with the entire torque and run for 336 hours, without any running-in process. The rotational speeds of the tested worms were:

n_1 = 400; 650; 1,030 and 1,470 1/min.

The torque varied from 1.0 to 1.75 times the nominal torque that is given by the gear manufacturer (Ref. 7). Cracks on the worm flanks were tested on larger gear sets with a center distance of a = 250 mm, a gear ratio of i = 39:2, a worm shaft arranged above the worm gear and a combined splash/circulating lubrication with an external oil cooling system. That test stand is shown in Figure 2.

The testing period is limited to a maximum of 1,650 hours. The rotational speeds are 1,500 and 2,200 1/min. During the tests, the applied torque exceeds the nominal torque 1.75 and 2.00 times. The employed lubricant for each case is a polyglycol called FVA-reference-oil PG4 (Ref. 4) with additive combination LP1655.

Test Results: Scoring

Figure 3 illustrates a worm gear damaged by score marks. Compared to new, never-run worms, the flanks show a rough surface within the area of contact. These score marks are transferred during operation to the flanks of the worm wheel and cause excessively increased wear that often leads to a premature failure of the entire gear set.

In order to register the amount of scoring damage, measurements of the surface are carried out in the complete mating area of the worm shaft. The measurements are taken in the radial direction, perpendicular to the expected score marks (Fig. 4).

In the radial direction, parts of the teeth are separated into foot, center and tip. Tests with a low rotational speed of n_1 = 400 1/min and 1.25 times the nominal torque show the largest scoring damage. The distribution of the measured arithmetic mean roughness R_a after testing is given with Figure 5. The measured values for each position from the beginning to the end of the contact area are plotted. The roughness of the flanks in the initial state is the standard of comparison. New worms have an average arithmetic mean roughness of R_a = 0.4 µm.

The distribution shown is typical for worms that are damaged by score marks. The greatest roughness always occurs at the end of the contact area close to the tip of the tooth. Towards the beginning of the mating area, the values of the roughness decrease. Similar tendencies can be observed in the center of the teeth, but the maximum values are lower. In the area of the foot, the measured values scatter, but they reach comparatively large values.

Comparative measurements of the worm shaft and the worm wheel show a good representation of the scoring damage of the worm flanks by measurements at the wheel tooth center. At this point, the smallest lubricant film thickness and the smallest relative motions directed toward the height of the tooth occur during operation between worm and wheel.

Score marks of the worm are reflected onto the center of the wheel teeth. Therefore, score marks at the wheel are suitable for the qualitative description of the scoring damage at the worm flanks. Figure 6 shows the measured arithmetic mean roughness at the wheel after separate test runs with different loads. All tests were executed with case-hardened worms made with 16MnCr5 steel and wheels made of GZ-CuSn12Ni bronze.

The test results show a significant dependence on rotational speed and torque. The amount of scoring damage increases with an increase in the torque applied and decreases with the rotational speed of the worm shaft (Fig. 6). On the one hand, increased load leads to an increased scoring damage. On the other hand, an increased rotational speed leads to less scoring. The strongest scoring damage can be observed at rotational speeds of n_1 = 400 1/min. At rotational speeds of more than n_1 = 1,030 1/min, no score marks result, even in the case of high overloads. The roughness of the flanks after testing is almost the same as in the beginning. The arithmetic mean roughness represents the amount of scoring damage.

A regression analysis quantifies the dependence of the expected arithmetic mean roughness on the worm wheel on different loads as rotational speed n_1, torque T_2 and oil sump temperature ϑ_S by four coefficients a_{1-4}.

$$R_{a,R} = a_1 + (a_2 - a_3 \cdot n_1 + a_4 \cdot \vartheta_S) \cdot T_2 \geq 0\,\mu\text{m} \quad (1)$$

Figure 7 shows the expected arithmetic roughness $R_{a,R}$ after application of Equation 1. A data map shows the expected scoring damage for the examined material-lubricant combination depending on torque and rotational speed.

As observed during the tests, the roughness increases with increasing load and decreasing rotational speed. Measurements during the testing reveal an increased wear for $R_{a,R}$ = 1–2 µm, and excessively increased wear if greater roughness applies. In some cases, the measured wear exceeds the values precalculated by DIN 3996 (Ref. 3) up to 20 times. For this reason, an arithmetic mean roughness above R_a = 2 µm has to be particularly regarded as critical. For operation with constant torque directly after gear set assembly, the loads should be chosen in a way that the expected arithmetic mean roughness stays below 1 µm, in order to avoid damaging score marks.

The presented approach can only be used to predict the behavior of the tested material/lubricant combination and the given geometry of the gearset. A prediction for operating points which are not represented by the examined range of torque and rotational speed is highly uncertain and not verified by practical investigations. A transfer of the results to different sizes and another tooth geometry just by conversion of the dependent factors n_1, T_2, ϑ_S to other factors such as sliding velocity v_{gm} and mean contact stress σ_{Hm} lack of test results for these conditions.

Methods to Avoid Score Marks

Scoring on the worm flanks can be avoided by the use of PVD-coated worms such as those coated with BALINIT C (Ref. 1) or the use of the additive GH6. Compared to the basic test runs, even higher torques can be applied. No score marks appear during these tests. Concerted oil changes after 48 and 144 hours help to reduce the scoring damage. However, scoring cannot be avoided completely by this particular means.

Compared to the basic gear sets, no

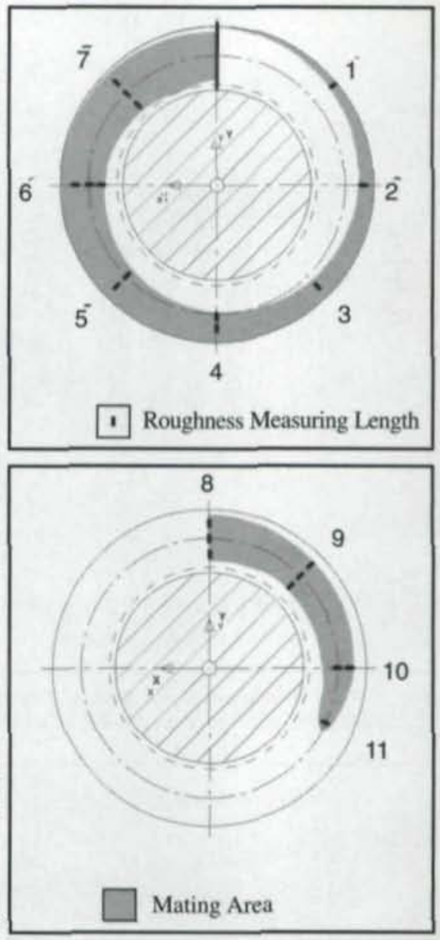

Fig. 4—Positions where measurements of the surface are taken to represent scoring damage.

Prof. Dr.-Ing. Wolfgang Predki
is the head of the chair of mechanical components, industrial and automotive power transmission at Ruhr University, located in Bochum, Germany. The chair's research focuses on wear optimization of worm gears, plastic and sintered worm gears and bronze optimization.

Prof. em. Dr.-Ing. Friedrich Jarchow
is the former head of the chair of mechanical components, industrial and automotive power transmission at Ruhr University.

Dr.-Ing. Ralf Dinter
is employed at Winergy AG, a leading provider of drive systems for wind turbines, located in Voerde/Friedrichsfeld, Germany. Winergy AG is a subsidiary of A. Friedr. Flender GmbH, based in Bocholt, Germany.

Dipl.-Ing. Alexander Rhode
is a research assistant at the chair of mechanical components, industrial and automotive power transmission at Ruhr University. His work focuses on the investigation of large scores on worms.

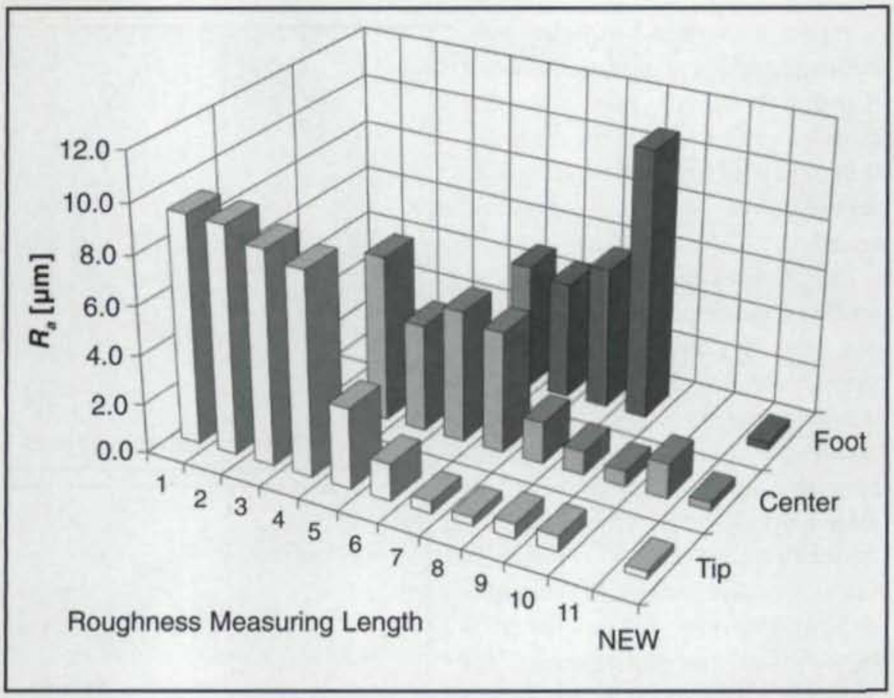

Fig. 5—Arithmetic mean roughness after testing (336 hours), n_1=400 1/min, T_2 = 1.25 • T_{2N}, 16MnCr5 case-hardened/GZ-CuSn12Ni.

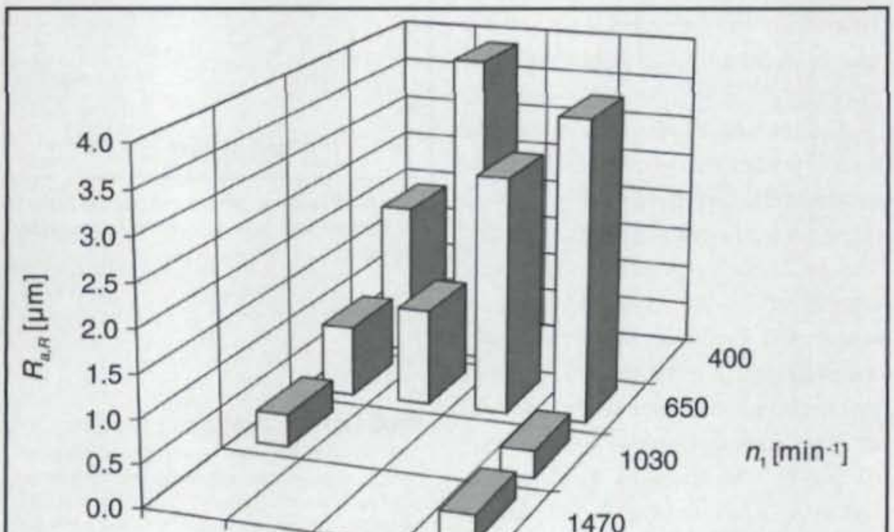

Fig. 6—Arithmetic mean roughness of the wheel after 336 hours.

improvement should be expected by the application of polished or crowned worms made of 16MnCr5 case-hardened steel. Spalling can be observed within the nitrided fringe of gas nitrided worms.

Test Results: Cracking

Radial cracks on the flanks of case-hardened worms can be encountered on gear sets with center distances above a = 200 mm, but they predominantly occur with center distances above a = 400 mm. High sliding speeds and incomplete starting contact patterns lead to high specific loads on the tooth flanks of these gear drives. For economical bench tests, gear drives of the size a = 250 mm were examined. These drives were charged with overloads up to twice the nominal torque.

Figure 8 shows a bar chart that sums up the results of several tests. The testing period is represented by the length of each bar. Different hatching indicates several defects on the worm flanks. The employed worm materials as well as the hardening processes are given with this figure.

The nominal torque must be exceeded by far to produce cracks. High loads lead to heavy pitting and, in some cases, excessive wear on the worm wheels. The cracks on the worm flanks always occur at the end of the mating area and show a radial alignment. There are two different areas for the origin of the cracks and their direction of growth. On the one hand, cracks start at the inner delimitation of the contact field with a growth direction towards the tip of the worm tooth (Fig. 9). On the other hand, cracks start at the tip and grow towards the tooth (Fig. 10). For both cases, the origin of the cracks is located within an area of disadvantageous lubrication conditions. After the tests, a local transfer of bronze can be observed in these areas.

Theoretical examinations (Refs. 2, 6) show the smallest lubricant film thickness at the inner delimitation of the worm mating area. Compared to other areas on the flank, higher friction factors apply for this region. The combination of high friction factor and the existing speeds lead, particularly towards the end of the mating area, to high temperatures on the flank.

Cracks that start at the tip of a worm tooth can be observed if large pitted areas are located on the wheel teeth and increased wear commences. The tooth face tip of the worm "digs" into the foot of the wheel tooth. The development of a sufficient lubricating film in this area is restrained by the sharp-edged tip of the worm tooth and the prevailing conditions of motion.

A theoretical analysis of the mating process shows a contact or wear between the tip of the worm tooth and the foot of the wheel tooth at the end of the worm mating area, which corresponds to the test results.

As metallographic examinations

show, the flanks of the worm were stressed by very high temperatures within the mating area. The fringe texture is thermally influenced. Even rehardening of the flank surfaces occurred. Rehardening requires temperatures above the austenite temperature of at least a_{Cl} = 723°C.

Internal stress analyses reveal that the loads applied to the worm flanks lead to high tensional internal stresses within the fringe. A new worm shows compressive internal stresses within the same areas.

The change in the state of internal stresses by high surface temperatures is shown in Figure 11. In this example, there is no internal stress at the beginning. A short application of a temperature field to the surface of a part causes compressive stresses within areas close to the surface because a free, temperature-caused extension is prevented by the surrounding colder areas. An increase of the temperature causes higher compressive internal stresses. If these stresses reach the hot-strain limit, permanent strains occur. The value of the hot strain-limit depends on the temperature. After removal of the thermal stress, the deformed area cools down and the strains are saved as tensional internal stresses. Hertzian contact stresses and tangential loads caused by friction promote this effect. If the local strength of the material is exceeded by tensional internal stresses, the growth of a crack commences.

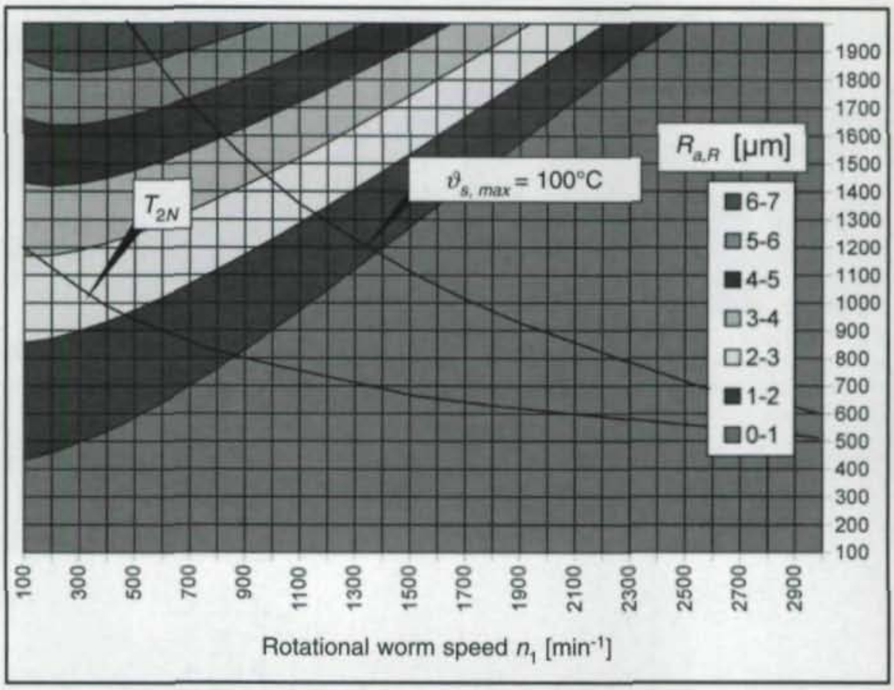

Fig. 7—Estimated scoring damage, calculated by Equation 1. Gear set: a = 100 mm, i = 20.5, 16MnCr5eh/GZ-CuSn12Ni, operation with nominal load, no running-in, nominal torque T_{2N} taken from manufacturer data (Ref. 7).

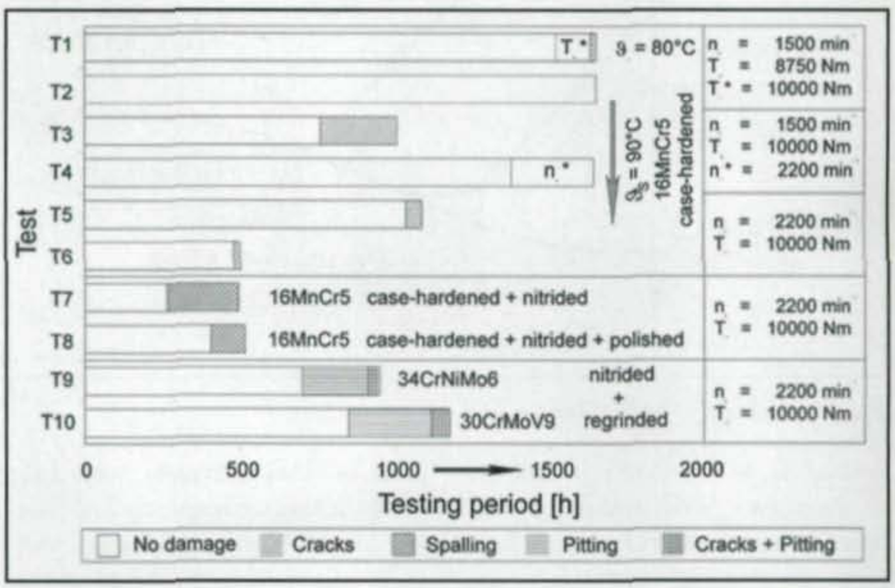

Fig. 8—Test results cracking. Wheel is GZ-CuSn12Ni; lubricant: FVA-PG4 + LP1655

Test Conclusions

The nominal torque has to be exceeded by far to produce cracks on the worm flanks. For this reason, these defects should not be expected under normal working conditions with worm gear drives of the tested size. The defects are caused by high thermal loads in combination with a local transfer of bronze. In particular, cracks occur in combination with heavily pitted worm wheels.

That is another reason why pitting should be avoided. Gas nitrided worms tend to spall within the nitrided layer.

In order to reduce the risk of cracks on case-hardened worms, the specific load on the flanks should be reduced and the load-capacity against scuffing should be increased. In general, this can be reached by the following means:

• Largest possible starting contact pattern;

• Fast running-in by use of a bronze with low strength in combination with a mineral oil, subsequent oil change and use of a more efficient polyglycol;

• Use of a lubricant with high load-capacity against scuffing in order to prevent local transfer of bronze;

• Prevention of pitting on the worm wheel (for precalculation, see Ref. 5).

Conclusions

This research project explores the critical loads of hardened worms that are combined with wheels made of bronze. Two different types of defects, large scores and radial cracks, are examined separately.

A map for score damage can be created. It shows that an increased amount of

Fig. 9—Worm taken from test T3. Origin of the crack at the inner delimitation of the contact field (cracks redrawn for better illustration).

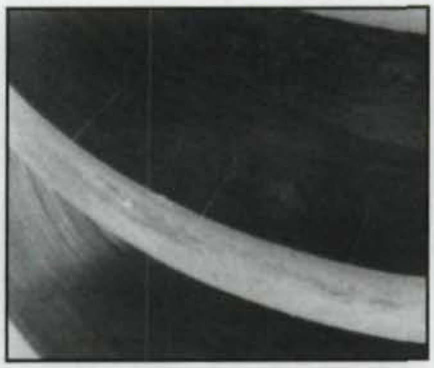

Fig. 10—Worm taken from test T1. Origin of the crack at the tip of the tooth.

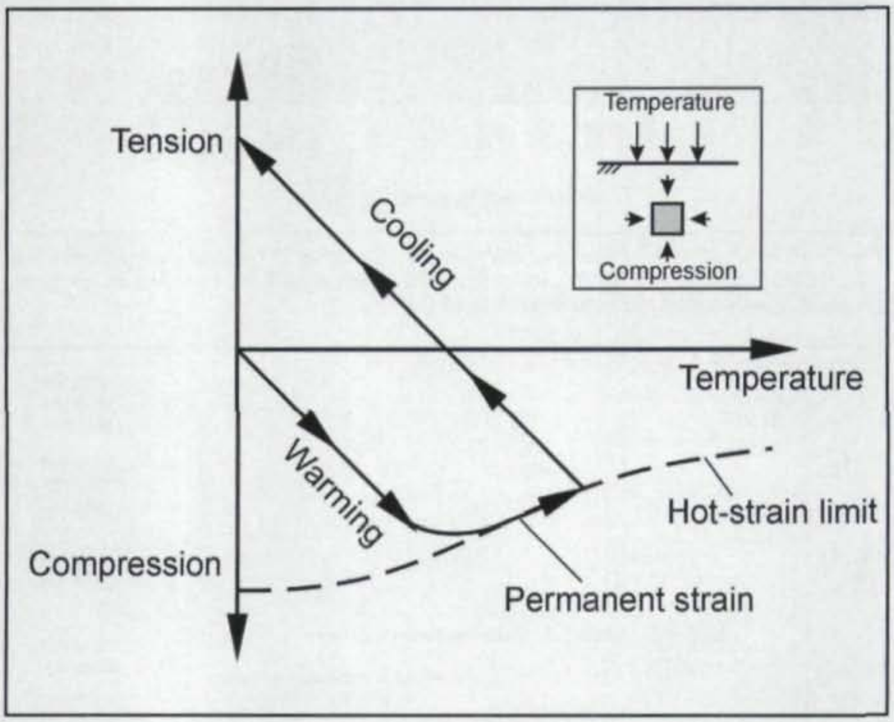

Fig. 11—Changes of internal stresses by thermal loads.

scoring is to be expected with an increased load. An increase in rotational speed reduces the expected damage. However, even high overloads do not produce score marks if high rotational speeds apply. An effective way to prevent scoring is the use of PVD-coated worms or the use of a lubricant with the additive GH6.

To generate cracks on the worm flanks, the nominal torque must be exceeded greatly. For this reason, cracks are not to be expected under normal working conditions with worm gear drives of the tested size. The defects are caused by high thermal loads in combination with a local transfer of bronze. The origin of the cracks is located within areas of disadvantageous lubrication conditions and consequently high thermal loads. Material tests showed thermally-influenced fringe texture and, in some cases, even zones where rehardening occurred.

Internal stress analyses indicate a change from initially compressive to high tensional internal stresses, caused by high flash temperatures. These stresses lead to cracks, if the local strength of the material is exceeded. In particular, cracks occur in combination with heavily pitted worm wheels. That is another reason why pitting should be avoided.

Further information can be obtained from the final report on research project 237 of the FVA (Ref. 5). ○

This paper was printed with the permission of the publisher from VDI-Gesellschaft Entwicklung, Konstruktion, Vertrieb (Ed.): International Conference on Gears, Vol. 1. VDI-Berichte 1665. Düsseldorf: VDI-Verlag 2002, pp. 435–449.

References

1. Balzers AG: "Firmenschrift", *Der Weg zu zuverlässigeren Bauteilen*, Liechtenstein 1993.
2. Bouché, B.: *Reibungszahlen von Schneckengetrieben im Mischreibungsgebiet*, Dissertation Ruhr-Universität Boch-um. 1991.
3. DIN-Entwurf 3996: *Tragfähigkeitsberechung von Zylinder-Schneckengetrieben mit Achsenwinkel Σ=90°*, Entwurf 1/95.
4. FVA-Forschungsheft 316: *Synthetische Referenzöle, Datensammlung für Syntheseöle*, 1990.
5. FVA-Arbeitsblatt zum Forschungsvorhaben Nr. 12/IV: *Versuche zur Grübchentragfähigkeit von Schneckengetrieben*, Stand Juni 1996.
6. FVA-Forschungsvorhaben 237. *Schneckentragfähigkeitsgrenzen ermitteln und erhöhen*, Heft 518 der Forschungsvereinigung Antriebstechnik, 1996.
7. Katalog der Firma Thyssen: *MUTAX Schneckenradsätze*, 1-750.
8. Klüber Firmenschrift: *Klübersynth GH6-Öle*, Produktinformation 5.118d, Ausgabe 03.93.
9. Predki, W.: *Hertz'sche Drücke, Schmierspalthöhen und Wirkungsgrade von Schneckengetrieben*, Dissertation Ruhr-Universität Bochum, 1982.

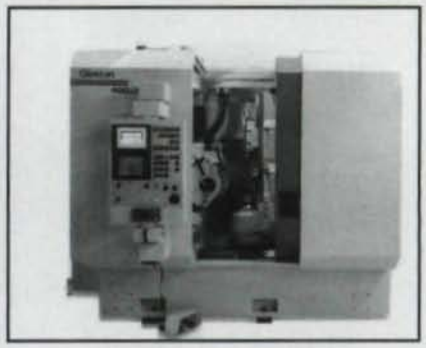

New Threaded Wheel Grinder from Gleason

The 400GX threaded wheel grinder from Gleason meets the need for finish grinding of gears for aerospace and other applications up to 400 mm in diameter and 8.0 module.

According to the company's press release, improvements in overall cycle times have been achieved through use of direct drive spindles for the grinding wheel and worktable spindles. Grinding surface speeds of 60 meters per second are also possible.

The grinder was designed to conserve floor space and for ease of use by installing a FANUC CNC controller with a Windows-based software interface.

For more information, contact Gleason Corp. of Rochester, NY, by telephone at (585) 473-1000 or on the Internet at *www.gleason.com*.

New Gearhead from HD Systems

The CSF-XHJ Size 5 gearhead from HD Systems delivers 3 arc-minute positional accuracy in a package size that is 22 mm x 26 mm long.

The rated torque of the gearhead is 5 lb.-in. and the maximum torque can reach 24 lb.-in. The input of the gearhead provides a direct connection to any motor, according to the company's press release.

Available in gear ratios from 30, 50 and 100:1, the high precision miniature gearhead includes a shaft output.

For more information, contact HD Systems of Hauppauge, NY, at (631) 231-6630 or on the Internet at *www.HDSI.net*.

New Gearmotors from Oriental Motor Corp.

The V Series quiet AC gearmotor from Oriental Motor Corp. provides strengthened shafts that mate to a series of long life (10,000 hours) GV gearheads.

Among their noise reduction techniques are a special tooth process technology that removes machining marks of 1–2 microns from the surface of motor pinions, an optimized quiet running design and new assembly techniques that ensure high accuracy assembly down to the micron level.

According to the company's press release, these gearheads achieve a threefold increase in maximum permissible torque levels. Output power levels of 6W, 15W, 25W, 40W and 60W are available, depending on motor frame size. Induction, reversible and electromagnetic brake motors are available as options.

For more information, contact Oriental Motor U.S.A. Corp. of Torrance, CA, at (800) 406-7484 ext. 836 or on the Internet at *www.orientalmotor.com*.

New Gearboxes from ZF Great Britain

The Graessner range of bevel gearboxes and gear sets is designed for power transmission and automation applications.

With a 98% efficiency rate, the range has graduated performance with units that offer superior precision, high torque and rigidity, and excellent levels of mounting flexibility.

The ValueGear is the entry-level unit and designed for OEMs. This product is packed with synthetic grease for lifetime lubrication and integrates "T" slots that provide adaption possibilities for mounting.

PowerGear has a rigid design and an optimized gear tooth contact pattern of 4,800 N-m torque performance from the smallest size envelope. These gearboxes require no external shaft couplings or flanges, enabling the user and OEM to save on both installation space and external equipment costs.

For more information, contact ZF Great Britain of Nottingham, U.K., by e-mail at *rob.pearson@zf-group.co.uk* or on the Internet at *www.zf-group.co.uk*.

Tell Us What You Think . . .
Visit *www.geartechnology.com* to
- **Rate this column**
- **Request more information**
- **Contact companies mentioned**
- **Make a suggestion**

Or call (847) 437-6604 to talk to one of our editors!

The Two-Sided-Ground Bevel Cutting Tool

Hermann J. Stadtfeld

Introduction

In the past, the blades of universal face hobbing cutters had to be resharpened on three faces. Those three faces formed the active part of the blade. In face hobbing, the effective cutting direction changes dramatically with respect to the shank of the blade. Depending on the individual ratio, it was found that optimal conditions for the chip removal action (side rake, side relief and hook angle) could just be established by adjusting all major parameters independently. This, in turn, results automatically in the need for the grinding or resharpening of the front face and the two relief surfaces in order to control side rake, hook angle and the relief angles of the cutting and clearance side. Figure 1 explains the nomenclature of the process-relevant angles on a cutting blade for a face cutter head. The effective hook angle was also manipulated to control the bias condition of the tooth contact, which seemed to make it impossible to avoid front face grinding, since the front face differs from one job to the next.

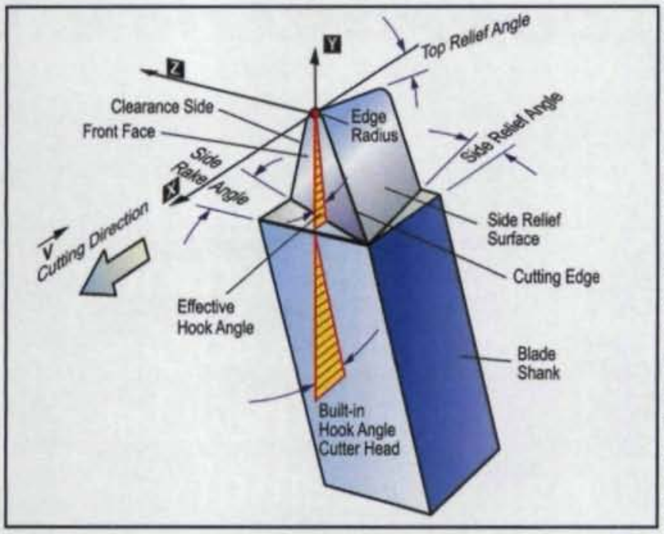

Figure 1—Process-relevant angles on a bevel gear cutting blade.

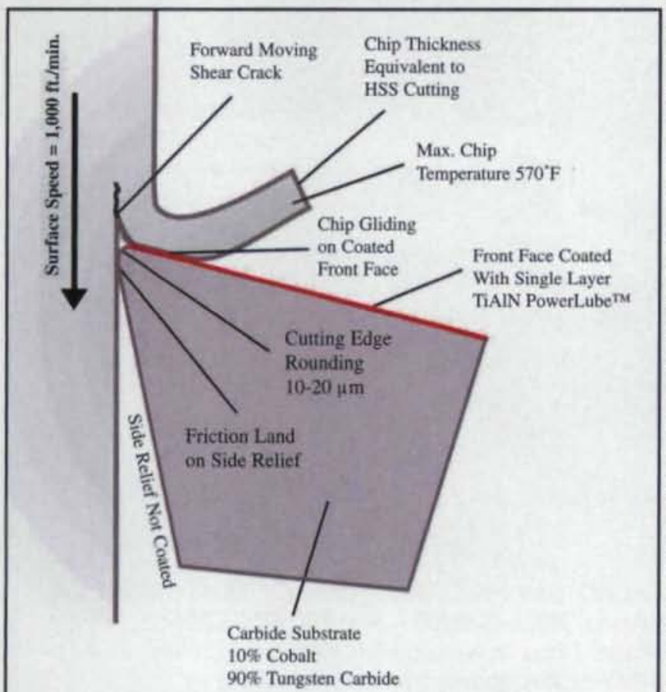

Figure 2—Chip forming mechanisms and specifications.

The face hobbing cutter head has the following design specifications:

- Slot radius
- Slot offset
- Number of blade groups
- Blade spacing
- Built-in hook angle
- Cutter height

At the time, it seemed to be impossible to replace the bias control using hook angle changes by other geometric alterations in blade or cutter head. Gleason Corp. found that a cutter head offset that allows for a permanent front face along the blade shank could be chosen. This would accommodate a wide range of different gear set designs with small deviations from the theoretically optimal side rake angle. This relationship, together with an additional idea that also controls the bias condition, will be explained in the following sections and is the key for the two-sided sharpened cutting tool.

Three-sided sharpening not only introduces higher tool cost per manufactured part, it also prevents the application of a permanent coating on any of the active blade surfaces. The front face is the most exposed to friction, pressure and the heat resulting from the chip removal action. Therefore, a coating of blade front faces with a protective layer enhances tool life and allowable cutting speeds significantly. Coating of the side relief surfaces could also be considered, but shows far less improvement in the performance of the cutting process. In cases of carbide blades applied for high-speed bevel gear cutting, it was imperative to use coatings on the front face for protection of the carbide grid from deterioration. The mechanical effect of the friction as well as the temperature generated by it is isolated from the carbide by the protective layer. The coating reduces friction and has a high temperature resistance compared to the raw carbide material. Figure 2 schematically shows the chip forming action.

Figure 2 makes clear that the front face of the blade is exposed to compressive stress, friction and temperature. The cutting edge has its highest exposure in the metal removal process during the start of a cut, when it penetrates in the surface and plasticizes the steel, generating the forward moving shear crack that forms the chip. The corner around the cutting edge is partially relieved from the contact to the workpiece material as soon as the shearing of a chip begins. Instead of coating, the cutting edge can be rounded with a 10-micron radius. This reduces wear and chipping. Tool life similar to the case of an all-around coating can be achieved.

The Relationship between Cutting Velocity Direction and Effective Side Rake Angle

In face hobbing, each bevel or hypoid gear set requires a certain blade offset or offset angle. The offset angle δ_W determines the difference between the circumferential cutter velocity and the direction of the effective cutting velocity. The following formula shows all parameters that have an influence in the value of δ_W:

$$\delta_W = \arcsin[\, z_W \cdot m_n/2R_W \,]$$

where: z_W ... number of blade groups
m_n ... normal module
R_W ... radius, cutter center to calculation point on blade

The formula above shows that changes of the number of blade groups (starts), the module (or pitch) and the cutter radius influence the offset angle. Provided that the number of starts as well as the cutter radius cannot change in one given cutter design, the module or the size of the teeth to cut will have the only influence in δ_W. To establish a new cutter design, the average tooth size expected for that cutter is used to calculate the value of m_n, which leads to a number for δ_W. The relationship between tooth size and normal module is:

$$m_n = \text{circular pitch}/\pi$$

The conclusion of the formula relations above is an increased δ_W for a coarse-pitch job and a decreased δ_W for a fine-pitch job, where the average job that was used to design the face hobbing cutter requires exactly the nominal value of δ_W. Figure 3 gives an example.

Job #1 requires an offset 1, derived from δ_{W1}. Figure 3 also shows that the inclination between the cutter speed vector (circumferential velocity) and the relative cutting velocity (effective cutting velocity) is labeled δ_W. If a cutter head is designed according to the parameters of Job #1, then the blade slots have to be machined in the position of the upper blade. For easier explanation, a front face with no side rake angle was chosen; the cutting velocity vector is therefore perpendicular to the blade front faces in Figure 1. If a cutter with the same radius and an identical number of starts should be used to cut fine pitch Job #2, then it would be required to machine the blade slots with a much smaller offset 2 of the lower blade in Figure 3 into the cutter body. This would accommodate the smaller inclination

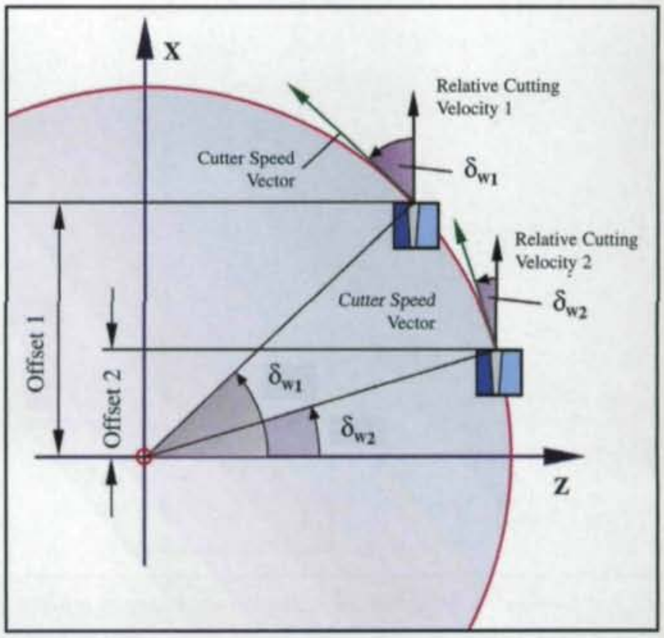

Figure 3—Optimal blade positions for two different-sized jobs using the same cutter radius and an identical number of blade groups.

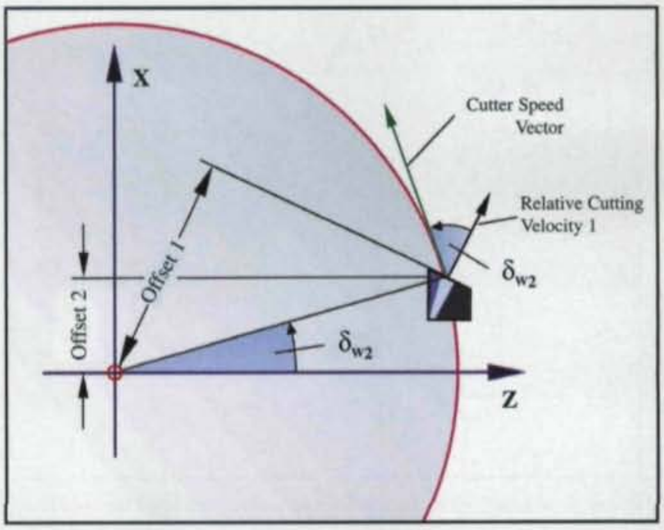

Figure 4—Blade with Offset 2 accommodates offset angle 1 by front face modification.

Dr. Hermann J. Stadtfled
started his career as head of engineering research and development at Oerlikon Geartec in Switzerland. From 1992–2002, he worked as vice president of research and development for The Gleason Works of Rochester, NY. Stadtfeld established Bevel Gear Industries (BGI) in Eisenach, Germany, in 2002.

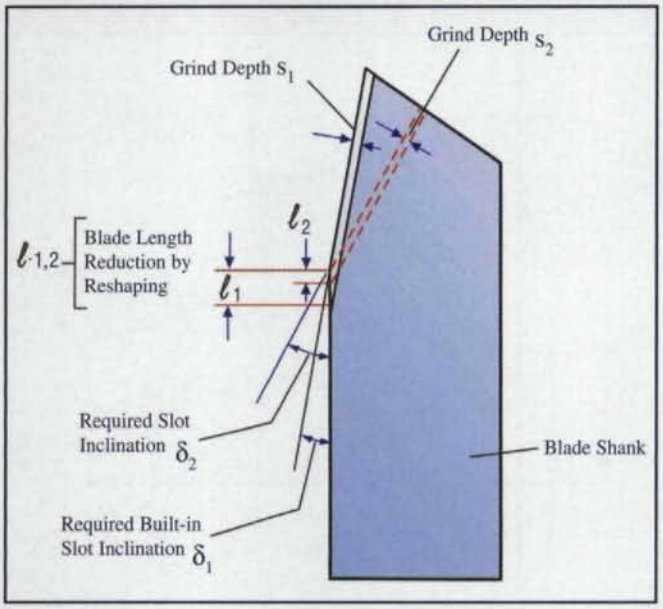

Figure 5—Blade length reduction after resharpening as a function of slot inclination.

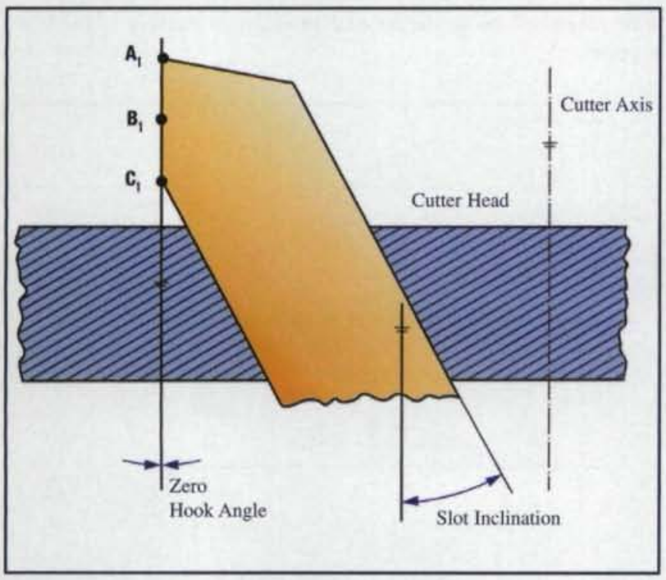

Figure 6—Cutter with slot inclination and zero effective blade hook angle.

between cutter speed vector and cutting velocity 2, δ_{W2}.

If a cutter head with slot offset 2 should be used to cut Job #1, a larger offset angle would be required, which presents a problem. This problem can be solved with a modification of the front face angle (side rake) as shown in Figure 4. The front face inclination in Figure 4 provides a front face orientation perpendicular to cutting velocity 1. The front face manipulation in Figure 3 simulates an offset, different to the built-in offset of the cutter head.

The three-face-ground blades have the freedom to change the front face orientation in a wide range and therefore realize correct front face orientation for a broad spectrum of pitch variation. But do the jobs that cut with one specific cutter size in fact vary from pitch significantly?

Relationship between Cutter Slot Inclination and Effective Hook Angle

All surfaces on a cutting blade need to have an inclination to the shank surfaces of more than 10°. Below 10°, the amount of material removal to clean up a worn cutting edge becomes too high. Figure 5 has a comparison of two different cutter slot inclinations. To result in a zero hook angle, the front face must be ground in about the same angle relative to the blade shank as the slot inclination of the cutter. Figure 5 demonstrates how a higher slot inclination allows a higher angle between front face and blade shank and leads to a smaller amount of blade length reduction.

Figure 6 shows a blade front face with a zero hook angle (connection of points A_1–B_1–C_1 is co-linear with cutter axis). The blade is held in the cutter slot that shows a significant slot inclination. After resharpening, the blade is moved in the slot against a stop in location A_1. The blade shank gets shorter with each resharpening, but the geometry above the face of the head remains identical throughout the life of the blade stick.

The angle between front face and blade shank is reduced, if a blade has a positive effective hook angle like shown in Figure 7. It is possible to increase the slot inclination in the cutter head within limits. The highest realized slot inclination is 20° in the Oerlikon Spirapid® cutter system (Ref. 1).

In most cases, a zero-effective hook angle is desired for an optimal cutting action. In this case, the relationship between the effective hook angle and the slot inclination of the cutter head is simple. It is only dictated by the requirement of an economical and effective resharpening. The 20° angle in the case of the Oerlikon Spirapid cutter system was a good choice for easy and economical resharpening of the stick blades. The measurement of 20° also left enough room for slight modifications of the effective cutting hook angle, e.g. to accomplish some bias modification of the flank form.

Blade System with Permanent Front Face

The Gleason Works introduced a new stick blade system in the 1970s, which did not require any resharpening or reconditioning of the front face (Ref. 2). Gleason called the cutter and the cutting system Relief Sharpened Roughing (RSR®) and later Relief Sharpened Completing System (RSR-C®). Figure 8 shows a three-dimensional graphic of an RSR-C blade with permanent front face. If resharpening of the blade front face is not required, then the rules for defining the cutter geometry are quite different. Since the effective hook angle now depends only on the pressure angle of the blade and the slot inclination in the cutter, the cutter slot is calculated in such a manner that the cutting edge with the highest possible pressure angle does not show a negative hook angle, when assembled in the cutter.

The blade in Figure 9 shows a constant cross section and was the next developmental step that converted the friction seating of the blades in the cutter in a positive form seating condition. Those blades are called PENTAC® because of their pentagon-shaped cross section (Ref. 3).

The variations of the hook angles from job to job caused by different blade pressure angles have only a very small geometrical influence on the generated flank surface in the single index face milling process. Those first order influences are compensated by a pressure angle correction.

To use the permanent-front-face blade system for the continuous face hobbing method causes two additional problems (Ref. 4). The effective side rake angle (first problem) might vary from job to job (discussed in Figures 3 and 4) caused by the different offset angles δ_W. The side rake problem can be solved with the blade in Figure 8 by defining a cutter slot offset that is exactly in the center of all jobs expected for the particular cutter. This means that a study of the different jobs cut with previous systems can tell very accurately what the average offset angle δ_W for a new cutter system should be and what the maximally accruing side rake deviations for the extreme jobs are. It is therefore possible to find an optimal slot position for each designed cutter with less than 2° variation of the effective side rake angle.

The second problem is the influence of the effective hook of the cutting edge on the generated flank surface. This influence is a flank twisting (bias effect). A flank twisting changes the direction of the path of contact and therefore causes a different orientation of the contact pattern, but also influences the motion graph amplitude significantly. In case of the three-sided-ground blades, it was possible to control the hook angle of the cutting edge such that it is always zero (or a predetermined desired angle). The following sections will explain the flank deviation effect by hook angle change analytically and present an interesting mathematical solution for this problem.

Analysis of the Geometric Effects to the Flank Form by Controlling the Front Face Orientation

The publications of Kotthaus (Refs. 1 and 5) teach that to maintain a sufficient side rake angle, especially to control the flank surface twist, the front face has to be variable in two angular directions, the side rake angle and the hook angle. The effective hook angle is the inclination around the normal cutter radius (Figure 10) between the cutting edge and the cutter head axis (Figure 7). The blade in Figure 7 is oriented such that the relative cutting velocity vector lies in the presentation plane. The effective hook angle is a function of the front face orientation with respect to the blade shank, as well as the angle of the blade slot in the cutter head (built-in hook angle) and the pressure angle of the cutting edge.

A change of the blade pressure angle has a direct influence onto the pressure angle of the manufactured tooth flank. A change of the hook angle in a face hobbing cutter blade caus-

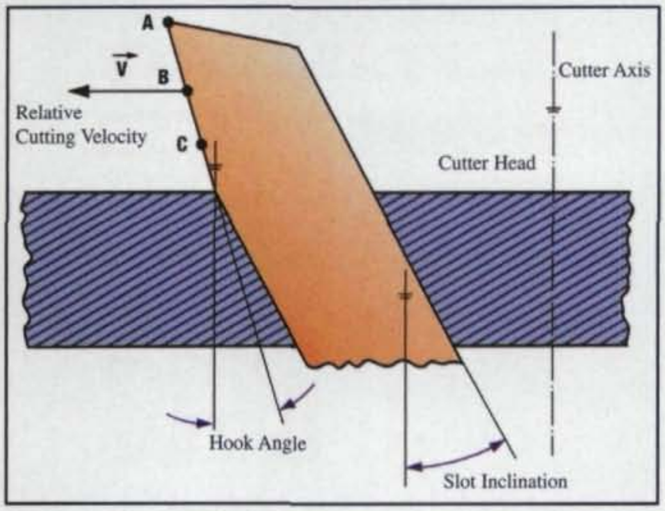

Figure 7—Cutter with slot inclination and positive effective blade hook angle.

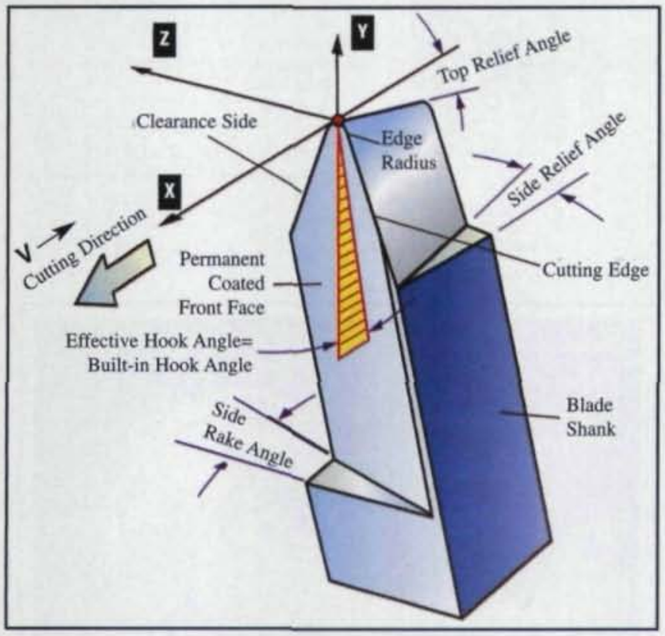

Figure 8—RSR-C stick blade with permanent front face and rectangular cross section.

es a flank twist and a change in profile crowning and pressure angle.

Figure 10 shows a blade with the Points A, B and C along a cutting edge that has a positive hook angle. The figure also shows a cutting edge without any hook angle (Points A_1, B_1 and C_1). The epicyclical path generated by A is different than the one generated by A_1. The curve associated with A_1 has a similar, but not identical, shape to the one generated by A. The two curves are inclined and shifted relative to each other in z-direction. That means the spiral angle of curve A decreases relative to A_1. The opposite happens for curve B relative to B_1.

The conclusion of the last paragraph is that the hook angle causes a positive flank twist between heel and toe. This, together with the already mentioned change in profile, represents crowning as a rather complex flank form modification.

The blade systems that allow a change of the hook angle use this freedom for flank form and contact movement (adjustability) optimizations. Studying the literature shows that the inventor of those systems found it physically impossible to allow the same optimizations by avoiding the individually controlled front face. All attempts during the past 30 years to develop a permanent front face cutter system with the same freedoms of the one with front-face-ground blades failed.

New SPIROFORM™ Cutter and Blade System

An interesting technical challenge was the attempt to develop a cutter and blade system that allows all the freedoms of the three-face-sharpened blade, yet using a blade that is shaped and sharpened on the two side relief surfaces only.

Finally, a discovery was made that relates the epicycloids, generated by different hook and side rake angles. The idea is to find the radial location of one point along the cutting edge of a given blade that lies on the same epicycloid, generated by a blade with different hook and side rake angle. It is assumed that the given blade consists of a permanent front face, no hook angle and a side rake that is constant along the shank. The hook angle of this system is created by an inclination of the slot in the cutter head.

Figure 11 shows the two different blade types with the roll circle-base circle kinematic "attached" to the front-face-sharpened blade.

The Points B and B_1 of the two blade types are identical (Figure 10). The problem to solve is to find the locations of the Points A_1 and C_1, along the existing front face of the simplified blade. The geographic height of the blade, with respect to the cutter head front face, remains constant.

To find the location of Point A_1, the epicyclical kinematics with roll circle and base circle are rotated clockwise until A contacts the front face of the new blade. This is the location of A_1. The movement from A to A_1 requires a rotation around the roll circle center, superimposed by a rotation around the center of the base circle. The relationships for the solution of this problem are shown in Figure 6 and expressed by the following formulas:

$$E_{X0x} + R_{B0x} = E_{X3x} + R_{B3x} \qquad (1)$$

or:

$$S \cdot \sin(-\Phi_0 - j + \delta_w) + R_{B0} \cdot \sin(\delta_w) = S \cdot \sin(-\Phi_0 - j + \delta_w + \varphi_w) + R_B \cdot \sin(\delta_w + \varphi_{Hook} + \varphi_c) \qquad (2)$$

where:

R_{b0x}...	x-Component of Cutter Radius Vector (Blade without Hook)
R_{b3x}...	x-Component of Cutter Radius Vector (Blade with Hook, rotated into zero Hook Plane)
E_{X0x}...	x-Component of Vector from Machine Center to

Cutter Center (Blade without Hook)

E_{X3x}... x-Component of Vector from Machine Center to Cutter Center (Blade with Hook, rotated into zero Hook Plane)

S... Radial Distance (Scalar of E_{X0x})

Φ_0... Cutter Phase Angle

j ... Swivel Angle

δ_w... Offset Angle (Face Hobbing)

R_{B0}... Scalar Cutter Radius (without Hook)

φ_w... Rotation of Cutter Center around Base Circle

R_B... Scalar Cutter Radius (with Hook)

φ_{Hook}... Angle between R_B and R_{B0}

φ_c... Rotation of Blade with Hook Angle around Roll Circle (Cutter Center)

Between φ_w and φ_c is the following relationship:

$$\varphi_w = \varphi_c/(1 + z_{generating\ gear}/z_{cutter}) \qquad (3)$$

where:

$z_{generating\ gear}$... Number of Teeth Generating Gear

z_{cutter} ... Number of Starts Cutter

Wanted is φ_w out of formula (2). The mathematical solution is conducted with an iteration algorithm. The difference between A_1 and A_2 is Δ. Δ is calculated as shown:

$$\Delta = | R_{B3} - R_{B0} | \qquad (4)$$

Δ is the displacement of the normal radius (along z-axis) of point A_2 to come to point A_1 that cuts the same epicycloid as point A. The epicycloid cut by A_1 will differ to some extent from the desired one, cut by A. The shown approach is the physically closest possible approximation, that infinitesimally observed still represents a mathematically precise solution. In practice, it causes differences over the entire flank surface of only a few microns and therefore can be neglected.

The analog scheme is applied to find point C_1 (Figure 7), a rotation of the epicyclical kinematic in counterclockwise direction brings C (Figure 7) to the front face of the new blade.

According to the above shown solution, any desired number of points along the cutting edge with one particular hook angle can be converted into a point on a cutting edge without hook angle or any other chosen hook angle.

Depending on the mathematical function of the new cutting edge (circle, ellipse or higher order), three, five or more points can be transformed from the original to the new cutting edge. Three points, one on the tip, one in the center and one on the end of the cutting edge, deliver a sufficient definition of the cutting edge function to capture the characteristics of the different front face hook angles.

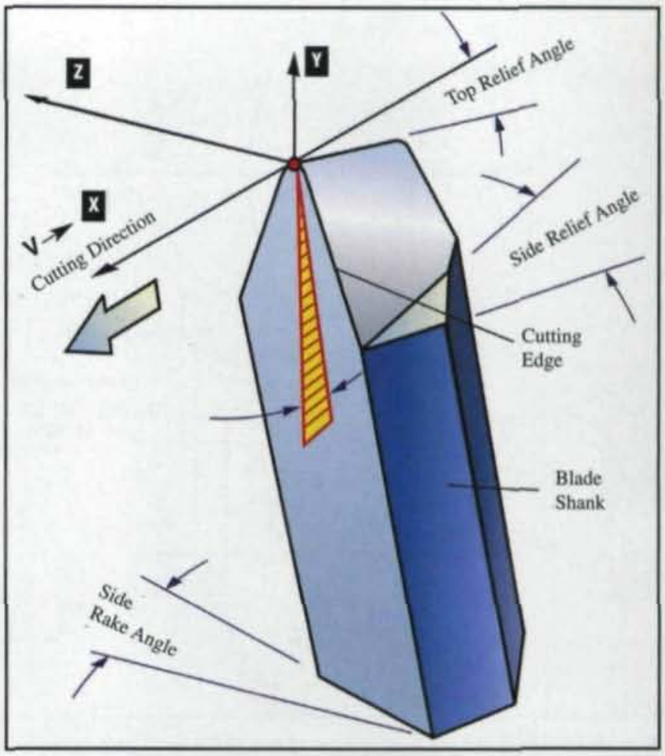

Figure 9—Pentac stick blade with permanent front face and pentagon-shaped cross section.

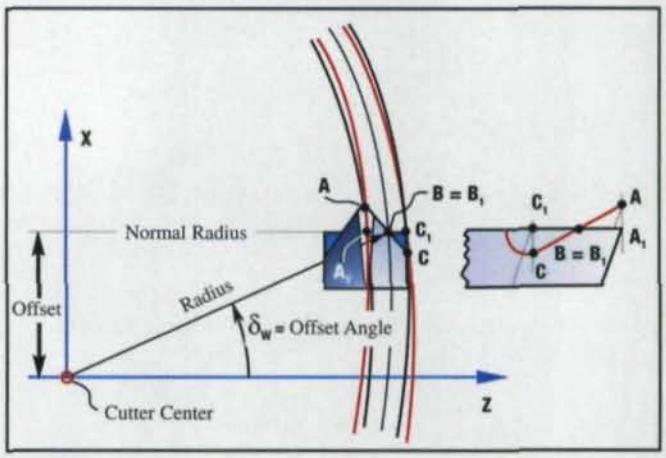

Figure 10—Relationship between hook angle and cycloidal path of different blade points.

The possibility to influence the blade spacing in the cutter head by grinding the front face of either inside or outside blade further back results in a tooth thickness or slot width change. The SPIROFORM blades can account for that feature, too. A tooth thickness adjustment is done by splitting the required amount and, for example, increasing the radius of the outer blade cutting edge and decreasing the cutting edge radius of the inner blade by half the amount each.

Summary

A method was found to convert a side relief and front-face-sharpened blade, held in a face hob cutter head into a blade that has a permanent front face and is profile shaped or re-sharpened

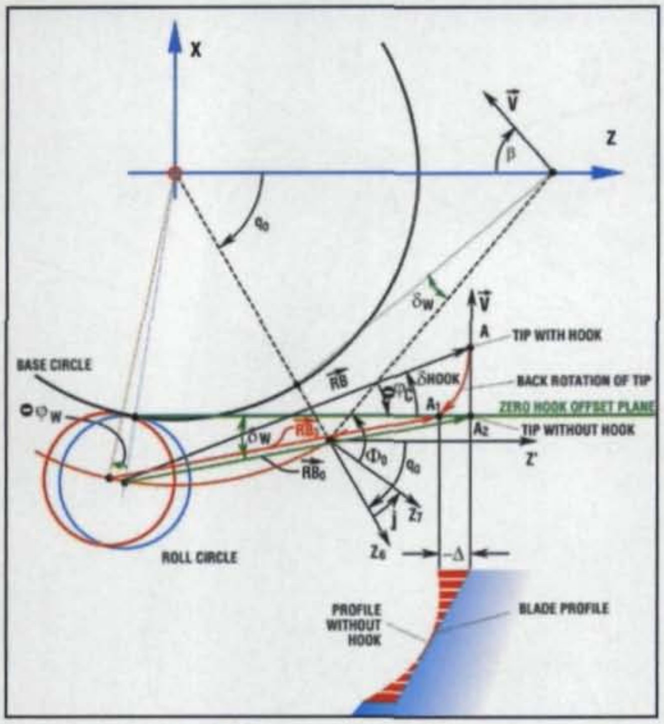

Figure 11—Epicyclical kinematics of two different blade types.

Figure 12—The Spiroform cutter head with a 160 mm radius and 13 starts.

Figure 13—Left side–conventional, right side–cut with Spiroform cutter head.

on the side relief surfaces.

The advantage of replacing the old style three-face-sharpened blade is in particular the permanent character of the front face and its coating. The new carbide high-speed cutting depends to a large extent on the correct front face coating. All gear sets, designed with a system using three-face-sharpened-blades can hardly be manufactured using high speed carbide cutting by replacing the high speed steel blades with carbide blades of the same geometry. To send a set of blades to a coating facility after resharpening requires more expensive carbide blades in storage and includes the cost of up to 100 recoatings of each blade. This procedure increases the tooling cost by a factor of eight.

The new SPIROFORM blades allow conversion of all older "three-face-ground" jobs into a two-face-sharpened blade system with a permanent front face coating. Gear sets do not have to be requalified after the conversion since the flank surface geometry stays identical to the original.

Figure 12 shows a photo of a SPIROFORM cutter with 160 mm radius and 13 starts. The SPIROFORM system uses no bottom blades. This provides a very solid and stiff cutter construction. The blades used (TRI-AC® or PENTAC) provide sufficient roughing action on the secondary cutting edges (clearance sides).

Front face coated blades provide good surface finish and improved productivity. The SPIROFORM blades are stepped in their building height, such that the tracks from outside blade and inside blade blend smoothly together in the root fillet.

Figure 13 shows an example of a conventionally cut ring gear. The gear to the right is cut using a SPIROFORM cutter and a Phoenix® free-form machine. Surface finish and root blends are superior for the new cutting system. Cutter heads and blades of the newly developed system are not limited to a certain machine tool brand, but can be applied on CNC bevel gear generators of The Gleason Works, Oerlikon Geartec AG and Modul-SU with no limitations.

References

1. Kotthaus, E. "Wirtschaftliches Herstellen von Spiralkegelrädern in kleinen und großen Serien", *Maschinenmarkt*, 83. Jg. Heft 73, Sept. 1977, Würzburg, Germany.
2. Ryan, A. and C. Thomas. Cutterhead Assembly for Gear Cutting Machines, U.S. Patent #4,060,881, December 1977.
3. Stadtfeld, H. *PENTAC: A New Cutter System for Face Hobbing and Face Milling*, Gleason publication, Rochester, NY, April 1998.
4. Krenzer, T. Cutter and Method for Gear Manufacture, U.S. Patent # 4,525,108, June 1985.
5. Kotthaus, E. End Cutter Head, U.S. Patent #3,760,476, January 1963.

Note: RSR® TRI-AC®, PENTAC®, SPIROFORM™ are trademarks of The Gleason Works.
Spirapid® is a trademark of Oerlikon Geartec AG.

ADVERTISER INDEX

USE RAPID READER RESPONSE to contact any advertiser in this issue
www.geartechnology.com/rrr.htm
Rapid Reader Response: It's FAST! It's EASY! It's ONLY ONLINE!

Advertiser	Page	Phone	E-mail	Internet
Accuspirals	46	(925) 285-3926	amar.pai@agileitpartners.com	www.accuspirals.com
AGMA	23	(703) 684-0211	gearexpo@agma.org	www.gearexpo.com
Ajax Tocco Magnethermic Corp.	3	(800) 342-1577	mmorrison@ajaxtocco.com	www.ajaxtocco.com
American Metal Treating Co.	45	(216) 431-4492	bruce@americanmetaltreating.com	www.americanmetaltreating.com
Arrow Gear Co.	4	(630) 969-7640	bevels@arrowgear.com	www.arrowgear.com
Ash Gear & Supply	46	(248) 374-6155	sales@ashgear.com	www.ashgear.com
ASI Machinery Co.	43	(704) 528-0902	asimachinery@aol.com	
A/W Systems Co.	39	(248) 544-3852		
B & R Machine and Gear Corp.	43	(800) 238-0651	inquirygt@brgear.com	www.brgear.com
Barit International Corp.	4	(847) 272-8128	people@barit.com	www.barit.com
Bourn & Koch Machine Tool Co.	46	(815) 965-4013	bournkoch@worldnet.att.net	www.bourn-koch.com
The Broach Masters Inc./Universal Gear Co.	8	(800) 563-3442, (530) 885-1939	sales@broachmasters.com	www.broachmasters.com
Crucible Service Centers	23	(800) 365-1185	crucible@crucibleservice.com	www.crucibleservice.com
Dr. Kaiser (S.L. Munson)	38	(800) 775-1390	info@slmunson.com	
Dragon Precision Tools Co. Ltd. (Greg Allen Co.)	40	(440) 331-0038	gallenco@msn.com	www.dragon.co.kr www.gallenco.com
Dura-Bar	6	(800) 227-6455, (815) 338-7800	sales@dura-bar.com	www.dura-bar.com
Fässler Corp.	42	(414) 769-0072	usa@faessler-ag.ch	www.faessler-ag.ch
Formax Precision Gear Inc.	46	(586) 323-9067		
Gear Motions Inc.	47	(315) 488-0100	ronwri@nixongear.com	www.gearmotions.com
The Gear Works-Seattle Inc.	45	(206) 762-3333	sales@thegearworks.com	www.thegearworks.com
Gleason Corp.	IFC, 47	(585) 473-1000	dmelton@gleason.com	www.gleason.com
Gleason Cutting Tools Corp.	1, 45, 47	(815) 877-8900	dmelton@gleason.com	www.gleason.com
The Gleason Works	46	(585) 473-1000	dmelton@gleason.com	www.gleason.com
Index Technologies Inc.	46	(440) 895-4627	gallenco@msn.com	www.gallenco.com
Indiana Tool/Indiana Gear	10	(574) 936-2112		www.itamco.com
Insco Corp.	29	(978) 448-6368	sales@inscocorp.com	www.inscocorp.com
Interstate Tool Corp.	46	(216) 671-1077		www.interstatetoolcor.com
ITW Heartland	29	(320) 762-8782	itwgears@rea-alp.com	www.itwgears.com
Koro Sharpening Service	46	(763) 425-5247	steve@koroind.com	www.koroind.com
LeCount Inc.	24	(800) 642-6713, (802) 296-2200	sales@lecount.com	www.lecount.com
Liebherr Gear Technology Co.	5	(734) 429-7225	info@lgt.liebherr.com	www.liebherr.com
mG miniGears North-America	17	(757) 627-4554	mg_usa@minigears.com	www.minigears.com
Midwest Gear Corp.	45	(330) 425-4419	sales@mwgear.com	www.mwgear.com
Midwest Gear & Tool Inc.	44	(586) 754-8923	rosscr@attglobal.net	
Nachi Machining Technology Co.	11, 46	(586) 263-0100	sales@nachimtc.com	www.nachimtc.com
Niagara Gear Corp.	45, 47	(800) 447-2392, (716) 874-3131	info@niagaragear.com	www.niagaragear.com
Perry Technology Corp.	IBC	(860) 738-2525	sales@perrygear.com	www.perrygear.com
Process Gear/Bengal Industries	41	(847) 671-1631	jhertl@processgear.com	www.processgear.com
The Purdy Corp.	25	(860) 649-0000	sales@purdytransmissions.com	www.purdytransmissions.com
Russell, Holbrook & Henderson Inc.	24	(201) 796-5445	sales@tru-volute.com	www.tru-volute.com
Star-SU Inc.	45, OBC	(847) 649-1450	sales@star-su.com	www.star-su.com

Performance of Skiving Hobs in Finishing Induction Hardened and Carburized Gears

Takeji Sugimoto, Akira Ishibashi, and Masataka Yonekura

In order to increase the load carrying capacity of hardened gears, the distortion of gear teeth caused by quenching must be removed by precision cutting (skiving) and/or grinding. In the case of large gears with large modules, skiving by a carbide hob is more economical than grinding when the highest accuracy is not required.

In the present investigation, carbide hobs with and without coated TiN layers were used for finishing hardened gears made from carbon and alloy steels. The gears to be skived were hardened by two different methods: induction hardening and carburizing. The induction hardened gears with a hardness of about 600 Hv can be finished easily by a carbide skiving hob without coating. However, the carburized gears with a hardness of about 750 Hv were very difficult to finish due to the severe flank wear and/or chipping at the cutting edges when a carbide hob without coating was used. However, when a carbide skiving hob with coated TiN layer on both the rake face and the flank was used, the tool life increased by a factor of about 10. Even with the skiving hob with the coated layer on the flank only, the tool life increased by a factor of about 7.

It was found that the tool lives of carbide hobs used for finishing hardened gears were governed by the flank wear and/or chipping which occurred on the fixed side (trailing side) of the cutting edges with a tool angle smaller than that of the other side (leading side). Therefore, in order to increase the lives of skiving hobs, it is strongly suggested to produce the coated skiving hobs with helical gashes, which give the same tool angle on both sides of the cutting edges.

Figure 1—Carbide hobs used for cutting tests.

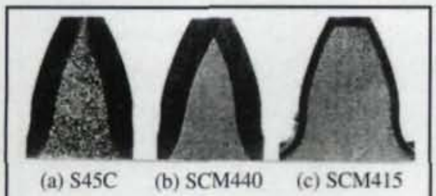

Figure 2—Transverse section of hardened teeth.

Table 1—Specifications of conventional and skiving hobs used in the experiments.							
Kind of hobs	Hob (A)	Hob (B)	Hob (C)	Hob (D)	Hob (E)	Hob (F)	Hob (G)
Module	8	8	8	8	8	8	8
Pressure angle	20°	20°	20°	20°	20°	20°	20°
Outside diameter (mm)	120	150	120	120	150	150	150
No. of gashes	9	10	10	10	12	12	12
Inclination of cutting edge	0°	0°	30°	30°	30°	30°	30°
Hob material	SKH55	P20	K10	M10	P20	P30	P30
Coating	TiN	none	none	none	none	TiN	TiN

Introduction

In order to increase the load carrying capacity of gear transmissions, it is desirable to use hardened gears. The quenching in the hardening process of the gears brings about heat treatment distortions, resulting in a reduction in the accuracy of the gears. To effectively utilize the gears, we must improve their accuracy after hardening, by using additional finishing operations such as skiving and/or grinding, honing, etc.

The highest accuracy can be obtained when the hardened gears are finished by grinding. One of the authors designed a gear grinding machine capable of making super precision gears with a mirror-like tooth surface using a CBN grinding wheel (Refs. 1–3). However, when the sizes of the gears are large, a long period of time is required to finish the gears by grinding. It is economical to finish the hardened gears by cutting using a carbide hob when the highest accuracy is not required.

Carbide hobs with special geometry (carbide skiving hobs) are very effective for accurately finishing hardened gears (Ref. 4). The lives of gear cutting tools can be increased by coating them with a thin, hard material (Refs. 5–7). The coating technique for the solid-type gear cutting tools made from high speed steel and carbide has progressed remarkably. Coated carbide hobs of the solid type and with a conventional geometry were effectively used for finishing low hardness gears with a small module (Ref. 8). However, it was very difficult to make the solid-type carbide hob economically when the modules of the work gears were large.

Brazed-type carbide skiving hobs without coating have been used for finishing hardened gears with large modules. However, a coated carbide hob with a sufficiently high accuracy for finishing hardened gears with large modules was not found in the market recently. The progress in both coating and brazing techniques makes it possible to produce high accuracy brazed carbide hobs with coating.

Recently, the authors have been able to obtain a coated skiving hob and conducted the cutting tests with some interesting results. The new, unpublished results obtained using non-coated carbide skiving hobs will be presented in this paper.

Cutting Tools and Test Gears

Specifications of Cutting Tools. Table 1 shows specifications of gear cutting tools (hobs) used for the present investigation. Hobs A and B are of the conventional type with a rake angle of 0° for the outside cutting edges. This means that the inclination angle of the side cutting edges is 0° and, therefore, no oblique cutting is conducted in finishing the tooth surface of the gears (Fig. 19a). Hob A is of the protuberance type and made from high speed steel. Hob B is of the carbide, brazed type with no protuberance.

Hobs C–G are of the carbide, brazed type with a special geometry for finishing hardened gears and are called "skiving hobs." No cutting action occurs at the outside edge of the hob blades. The inclination angle of the side cutting edges of these hobs is 30°, which corresponds to a rake angle of –30° in the case of the conventional hob. The whole tooth depth of skiving hobs was made smaller than that of conventional hobs to prevent cutting action at the tooth bottom of the gears to be finished. The carbide blades of Hob F were coated with a TiN layer with a thickness of about 5μm while those of Hobs C, D and E were not coated. The blades of Hob G were coated on the flank only. Figure 1 shows a conventional carbide hob (Hob B), a skiving hob without coating (Hob E) and a skiving hob with coating (Hob G).

Specifications of Test Gears. Kinds of materials and specifications of test gears are shown in Table 2. A 0.45% plain carbon steel (S45C) and a medium carbon alloy steel (SCM440) were used for induction hardening gears while low carbon alloy steels (SCM415 and SCM420) were used for carburizing gears. For cutting tests, spur gears with a module of 8, a pitch circle diameter of 208 mm and a face width of 60 mm were used.

Using the gear blanks with a hardness of about 200 Hv (normalized steel), rough-cut gears were produced by Hob A. The gears were hardened by induction hardening or carburizing.

For induction hardening, a partial coil was inserted in the tooth space and moved in the direction of tooth trace at a speed of about 300 mm/min. to heat over the two facing tooth surfaces. The tooth surfaces were heated to a temperature of about 1,250°K for the plain carbon steel and to a temperature of about 1,150°K for the alloy steel. Quenching of the heated teeth was conducted using water with some additives to prevent occurrence of quenching cracks on the tooth surfaces. After hardening, the gears were tempered at a temperature of about 470°K for two hours to obtain a Vickers hardness of about 600 Hv (Fig. 3).

The carburizing was conducted at a temperature of about 1,200°K in a mixed gas, which consisted of propane gas and alcohol. After carburizing for five-and-a-half hours, the temperature was decreased from 1,200°K to 1,120°K and quenched in non-soluble oil. After hardening, the gears were tempered for two hours at a temperature of about 470°K to obtain a hardness of about 750 Hv.

Figure 2 shows the transverse section of hardened gear teeth of test gears. Figure 3 shows the hardness distribution below the surface of the hardened teeth made from three different materials. The hardness was measured at an indenter load of 9.8 N. The maximum hardness of induction hardened gears is about 600 Hv and the thickness of the hardened layer is about 3 mm. The maximum hardness of carburized gears is about 750 Hv and the thickness of the hardened layer is about 1 mm.

The accuracies of test gears (rough cut gears) deteriorated appreciably by harden-

Table 2—Specifications of test gears and kinds of gear materials.

No. of teeth	Z = 26
Helix angle	0°
Face width	b = 60 mm
Material	S45C, SCM440, SCM415, SCM420
Hardness (Hv)	600, 600, 750, 750

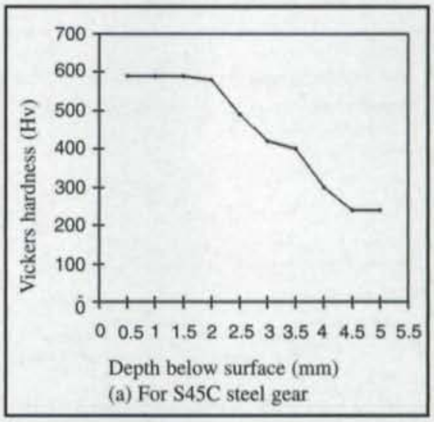

Figure 3a—Hardness of hardened teeth.

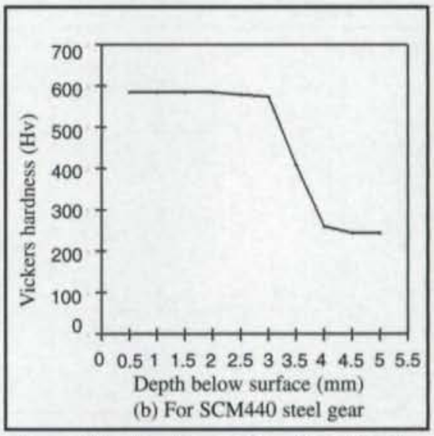

Figure 3b—Hardness of hardened teeth.

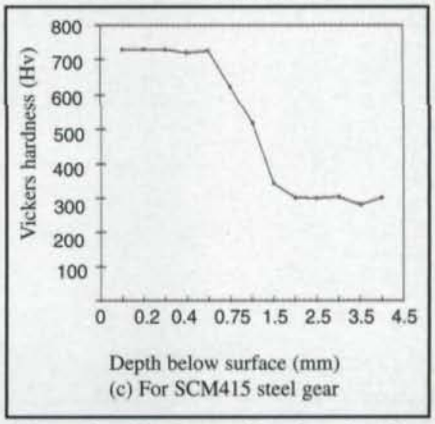

Figure 3c—Hardness of hardened teeth.

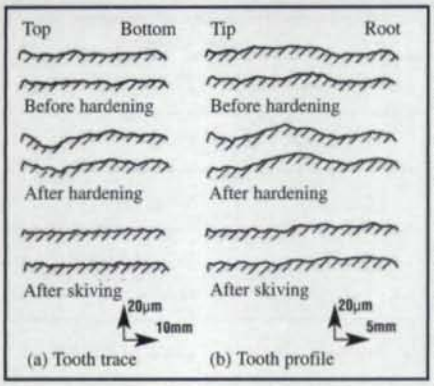

Figure 4—Tooth trace and profile errors of induction hardened gears.

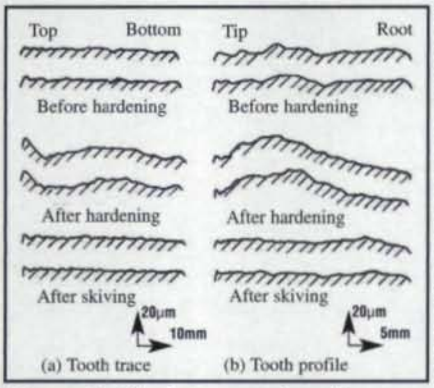

Figure 5—Tooth trace and profile errors of carburized gears.

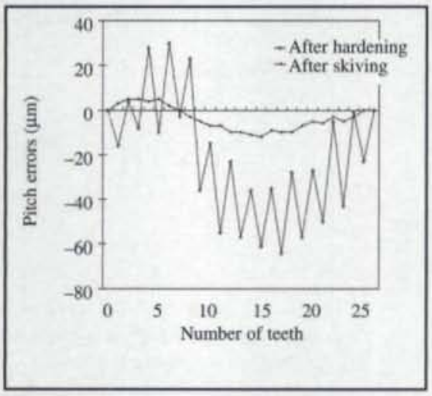

Figure 6—Pitch errors of induction hardened gears before and after skiving.

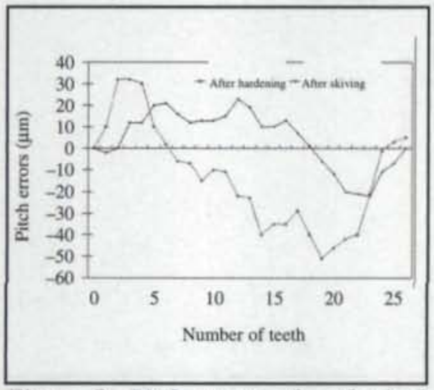

Figure 7—Pitch errors of carburized gears before and after skiving.

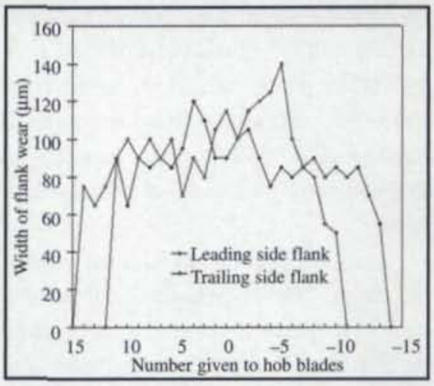

Figure 8—Wear width of all working blades of Hob E without coating used for finishing carburized gears.

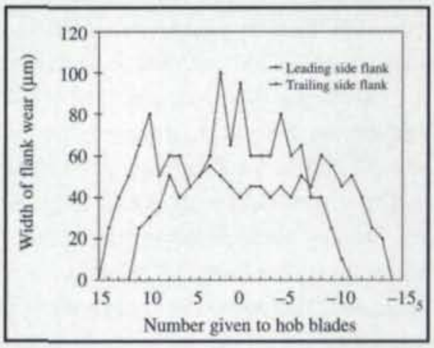

Figure 9—Wear width of all working blades of Hob F used for finishing carburized gears.

ing (Figures 4 and 5). Therefore, hard finishing by carbide skiving hobs becomes very important to economically improve the accuracy of the hardened gears.

Cutting Tests and Tool Wear

Hobbing Machine and Cutting Conditions. For rough and finish cutting of test gears, a hobbing machine with a capacity capable of finishing gears with diameters up to 1,000 mm was used. The machine was made by Kashifuji Co. Ltd. in Japan. Using Hob A made from high speed steel, rough hobbing of nonhardened gears was conducted under the following conditions: a cutting speed of 28 m/min., a hob feed of 2 mm/rev. and a final depth of cut 0.3 mm in the radial direction. The conditions used for skiving of the hardened gears were a cutting speed of 75 or 52 m/min., a hob feed of 2 mm/rev. and a depth of cut 0.3 mm. No cutting fluid was applied.

Changes in Accuracy of Test Gears. Figures 4 and 5 show the accuracies of the tooth profiles and tooth traces of test gears before hardening (after rough cutting), after hardening (before skiving) and after hard finishing (after skiving). For rough cutting, Hob A was used, while Hob F was used for hard finishing (Table 1). Figures 6 and 7 show the cumulative pitch errors of the test gears before and after skiving.

From Figures 4 to 7, it is understood that the decrease in the accuracy caused by the heat treatment was improved by hard finishing for both the induction hardened and the carburized gears.

Effect of Coating on Tool Life. When the coated Hob F was used for finishing the carburized gear at a cutting speed of 75 m/min. and a feed of 2 mm/rev., the flank wear width became greater than 0.2 mm after finishing a single piece of the test gear. Therefore, the cutting speed was reduced from 75 m/min. to 52 m/min. in the following experiments.

When a noncoated hob (Hob E) was used for finishing the carburized gears, the maximum wear width of the hob blades exceeded 0.05 mm after finishing only a single gear. Figure 8 shows the flank wear width on all working blades (side cutting edges) of carbide Hob E after finishing of two carburized gears. Twenty-three blades of the hob were used to finish the gears. The dark mark shows the flank wear width at the left side (leading side) cutting edges while the empty mark shows the wear width at the right side (trailing side) cutting edges.

When coated Hob F was used, 10 carburized gears could be finished before the flank wear reached about 0.1 mm. Figure 9 shows the flank wear width of all working blades of Hob F after finishing 10 carburized gears. Figure 10 shows the effect of the coating on the tool lives of carbide skiving hobs, indicating that the tool lives increased by a factor of seven when the coated hob was used instead of the noncoated hob.

In order to increase the tool lives, it is desirable to use a coated hob such as Hob F with the coated layer on both the rake face and the flank of the cutting edges. However, the coated layer on the rake face is removed completely when the worn cutting edges are sharpened by regrinding.

Recoating of the reground hob may bring about a reduction in the hob's accuracy. Therefore, additional cutting tests were conducted using a skiving hob with the coated layer on the flank only.

Figure 11 shows the flank wear width of all working blades of Hob G after cutting seven carburized gears. By comparing Figures 9 and 11, it can be seen that the coating on the flank only is effective. The tool life becomes shorter by about 30% when compared with that of the hob with the coated layer on both the rake face and the flank (Figure 10).

When Hob G was used for finishing the induction hardened gears with a hardness of about 600 Hv, the tool life increased appreciably in comparison with that of the noncoated hob. Hob G could finish 16 gears before the wear width reached 0.05 mm. Figure 12 shows the flank wear width on all working blades of Hob G after finishing 16 induction hardened gears.

Wear Pattern on Flank. Figure 13 shows wear patterns that were produced on the rake face and the flank of the representative blade of Hob F after cutting 10 carburized gears. Both the rake face and flank of this hob were coated by a TiN layer. Figure 14 shows wear patterns on the flank of Hob G after cutting seven carburized gears. This hob had the coated layer on the flank only. It was estimated that the flank wear on the right side cutting edge was increased appreciably by the occurrence of chipping at the cutting edge. The reason why the flank wear width at the trailing cutting edges is appreciably greater than that at the leading cutting edges is discussed in the next section.

Figure 15 shows wear patterns on the flank of Hob G after cutting 16 induction hardened gears. No chipping occurred at the cutting edges, and the wear width was very small, indicating the effectiveness of the coated layer on the flank. The difference in the wear widths on left side and right side cutting edges is comparatively small because the hardness of the induction hardened gears is lower by about 150 Hv than that of carburized gears, resulting in no chipping at the cutting edge.

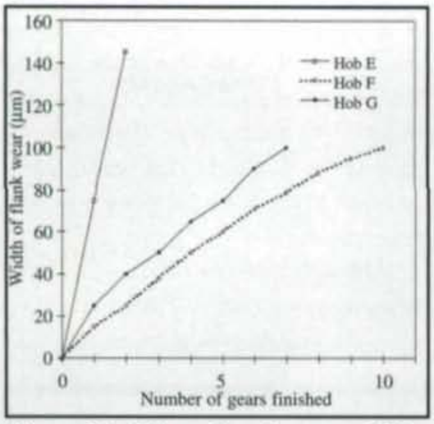

Figure 10—Effect of coating on tool life.

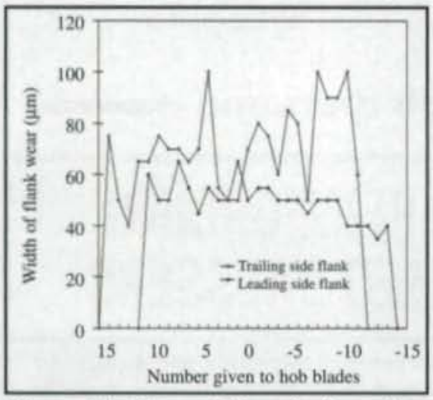

Figure 11—Wear widths of all working blades of Hob G after finishing seven pieces of carburized gears.

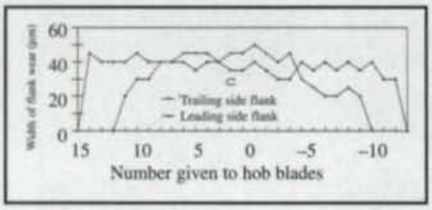

Figure 12—Wear width of Hob G after finishing 16 pieces of induction hardened gears.

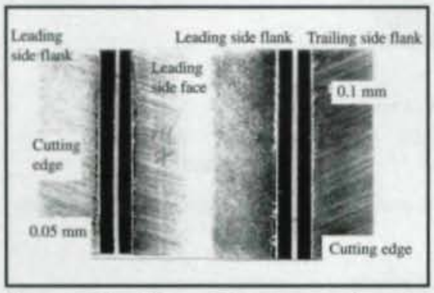

Figure 13—Wear patterns on rake face and flank of coated Hob F after cutting 10 carburized gears.

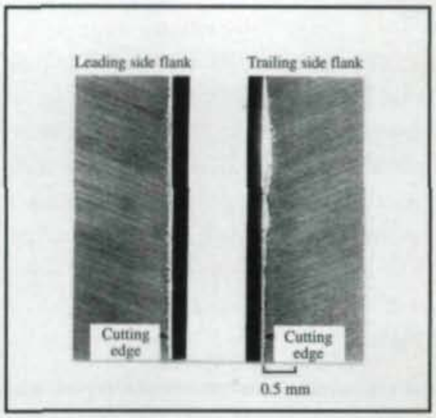

Figure 14—Wear patterns on flank of Hob G after cutting seven carburized gears.

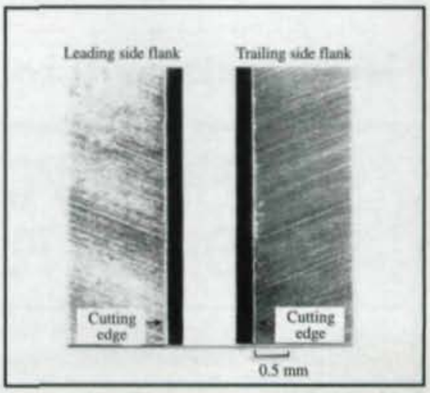

Figure 15—Wear patterns on flank of hob G after cutting 16 induction hardened gears.

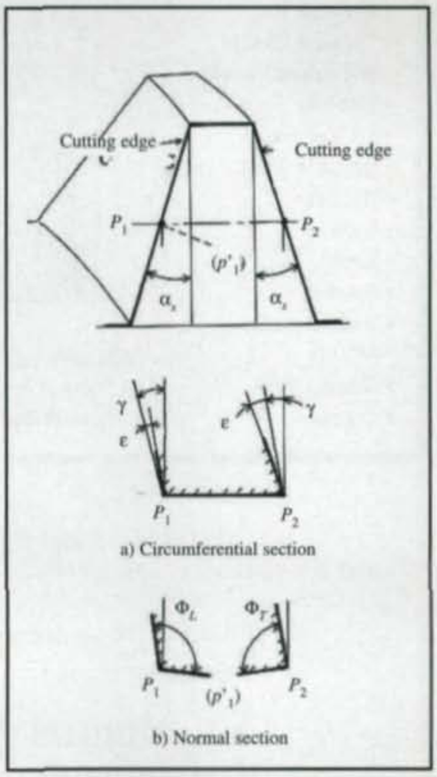

Figure 16—Tool angles of conventional hob with straight gashes.

Discussion

Difference in Wear at Leading Side and Trailing Side Cutting Edges. In the case of gear skiving, the volume of metal on the tooth surface removed by the trailing side cutting edges is almost the same as that removed by the leading side cutting edges. However, it should be noted that the experimental results shown in Figures 8, 9, 11 and 12 indicate that the flank wear at the trailing side cutting edges is greater than that of the leading side cutting edges. Chipping is also apt to occur at the trailing side. The reason for this may be ascribed to the type of gashes given to the hobs used in the present experiments.

Although there are two representative types of gashes utilized for gear cutting hobs, the straight type is commonly used

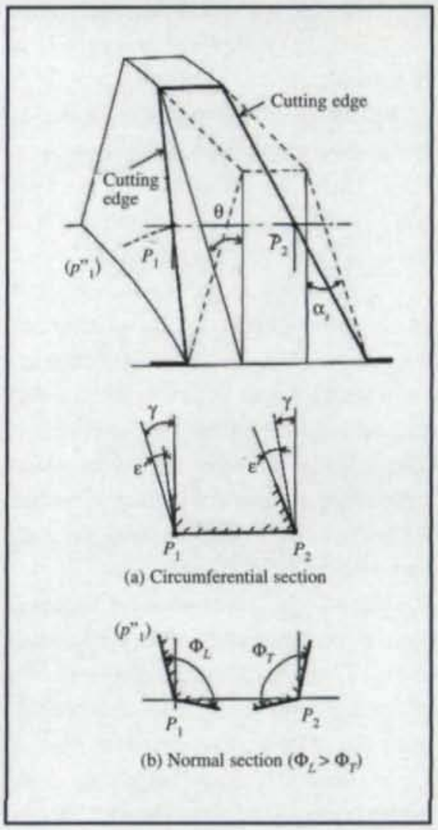

Figure 17—Tool angles of skiving hob with straight gashes.

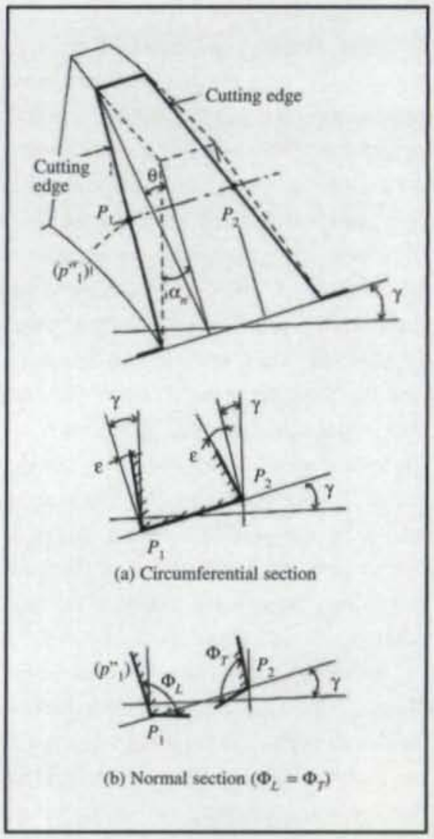

Figure 18—Tool angles of recommended skiving hob with a helical gash.

for the conventional hobs. This is because the accuracy of hobs with straight gashes can be improved with lower manufacturing costs in comparison with that of the hobs with helical gashes. Figures 16 and 17 show the geometrical characteristics of the hob blade in the conventional and skiving hobs.

Figure 17b shows a sectional view of the blade of a skiving hob with cutting edges on a right-hand helical thread and with a straight-type gash. The right-side cutting edge (trailing side cutting edge) gives a smaller tool angle than that of the left-side cutting edge (leading side cutting edge). The greater the tool angle, the smaller the chance of chipping at the cutting edge.

The maximum tool angle is obtained in the section normal to the cutting edge. The maximum tool ϕ_L for the leading side can be calculated from Equation 1 and the maximum tool angle ϕ_T for the trailing side is calculated from Equation 2.

$$\phi_L = 90^\circ + \Delta\phi + \gamma' \qquad (1)$$

$$\phi_T = 90^\circ + \Delta\phi - 2\gamma + \gamma' \qquad (2)$$

where,

$\sin\Delta\phi = (\sin\eta \sin\alpha_n - \tan\varepsilon / \cos\eta)\cos\alpha_n$

$\tan\eta = \tan\theta \cos\alpha_n$

$\tan\gamma' = \tan\gamma / \cos\alpha_n$

Although the process for deriving these equations is omitted due to lack of space, numerical examples are shown as follows. In the case of Hobs F and G, when given geometrical values (pressure angle $\alpha_n = 20^\circ$, lead angle of hob thread $\gamma = 3.6^\circ$, relief angle $\varepsilon = 3.7^\circ$, nominal rake angle $\theta = 30^\circ$) are introduced into Equations 1 and 2, $\phi_L = 98.7^\circ$ and $\phi_T = 91.4^\circ$ are obtained. For the conventional Hob B with $\theta = 0^\circ$ and $\varepsilon = 3.5^\circ$, $\phi_L = 90.6^\circ$ and $\phi_T = 83.3^\circ$ are obtained. These calculated values agree with the measured ones.

From these values for tool angles, it is clearly understood that the chipping hardly occurs on the cutting edges of the skiving hob with $\theta = 30^\circ$ because the maximum tool angle is greater by about 8° than that of the conventional carbide hob with $\theta = 0^\circ$.

The effect of the tool angle on the flank wear of the carbide hob becomes greater when the hardness of a gear is very high, as in the case of carburized gears (Figs. 8 and 9).

Method to Improve Tool Lives of Skiving Hobs. From the present experiments, it is estimated that the tool lives of skiving hobs can be increased when a skiving hob is designed to have the same tool angles for the leading and trailing sides. This is easily realized by changing the types of hob gashes. When the spiral angle of the hob gashes is made equal to the lead angle of hob thread, the maximum tool angles for the leading and trailing sides become the same and are calculated from Equation 3 (Fig. 18).

$$\phi_L = \phi_T = 90° + \Delta\,\phi \quad (3)$$

When the given geometrical values are the same as those of the above mentioned example excepting for the gashes, tool angle $\phi_L = \phi_T = 94.8°$ is obtained.

The authors estimate that application of coated skiving hobs with helical gashes is very important for finishing fully-hardened carburized gears economically, although with some increase in the manufacturing costs for the hobs.

Advantages Obtained by Oblique Cutting. When the skiving hob was used, the side cutting edge conducts intermittent oblique-cutting (milling) to finish the tooth surface, as shown in Fig. 19b. Although there are some fundamental investigations on the mechanism of the continuous oblique cutting (Refs. 9–10), many problems must be solved to obtain effective equations for calculating changes in the cutting force during the intermittent oblique cutting, such as in gear skiving. Moreover, there are practical problems. For example, the effects of oblique angle on the amount of tool wear, the shape of chips, etc. The authors are conducting some basic investigations to show the effect of intermittent oblique cutting on tool wear and the finished accuracy using a hobbing machine, and the carbide fly tools with and without coating. The results obtained will be published in the near future.

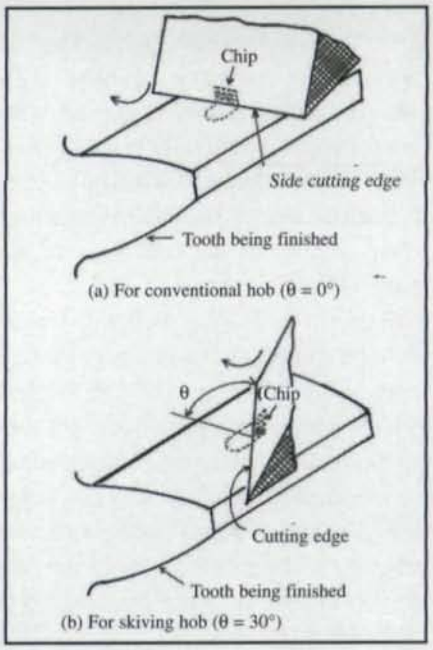

Figure 19—Oblique angle of cutting edges of the two different hobs.

Conclusions

The present investigation was conducted using six kinds of carbide hobs, and the following results were obtained:

1. Induction hardened gears with a Vickers hardness of about 600 Hv could be easily finished by a carbide skiving hob without coating.
2. Carburized gears with a hardness of about 750 Hv were very difficult to finish due to wear and chipping at the cutting edges when skiving hobs without coating were used.
3. When a carbide skiving hob with a coated TiN layer of about 5μm in thick-

ness was used, the tool life increased by a factor of 10 in comparison to the one without coating.

4. The skiving hob with a coated layer on the flank only was effective in increasing the tool life, especially in finishing induction hardened gears with a hardness of about 600 Hv.

5. The flank wear of the trailing side cutting edge was appreciably greater than that of the leading side cutting edge when the hobs were used for finishing carburized gears.

6. The reason for the difference in the wear is explained by calculating the difference in the maximum tool angles of the leading and trailing sides (Fig. 17).

7. It is estimated that the tool life of a skiving hob to be used for finishing fully hardened carburized gears can be increased by introducing coated hobs with almost the same tool angle for leading and trailing sides.

8. The tool angles for the leading side and trailing side cutting edges become the same value when the numerical value of the spiral angle of the hob is made equal to that of the lead angle of the hob tooth thread.

Acknowledgments

The authors express their thanks to the engineers of the machine shop at Kurume Technical College for their assistance in this investigation.

References

1. Ishibashi, A., S. Tanaka, and S. Ezoe. "Design and Manufacture of Precision Gear Grinder with CBN Wheel and Load Carrying Capacity of Gears Ground," *Bulletin of JSME*, Vol. 28, No. 238, 1985, pp. 718–725.

2. Ishibashi, A., S. Tanaka, and S. Ezoe. "Design and Manufacture of a CNC Gear Grinder Capable of Mirrorlike Finishing," *JSME International Journal*, Series III, Vol. 33, No. 2, 1990, pp. 245–250.

3. Ezoe, S. and A. Ishibashi. "High-Speed Mirrorlike Grinding of Precision Gears Using a Trial Gear Grinder with a CBN Wheel," *Proceedings of JSME International Conference on Motion and Power Transmissions*, 1991, pp. 207–212.

4. William, E. Loy. "Hard Gear Processing with Skiving Hobs," *Gear Technology*, March/April 1985, pp. 9–14.

5. Rech, J., M.A. Djouadi, and J. Picot. "Wear Resistance of Coatings in High Speed Gear Hobbing" *Wear*, No. 655, 2001, pp. 45–53.

6. Matuoka, H. and Y. Tuda, "Influence of Coating Films on Behavior of Crater Wear of Hobs in Dry Cutting," *Transactions JSME*, Series C, Vol. 67, No. 656, 2001, pp. 267–273.

7. Bouzakis, K.D., et al. "Gear Hobbing Cutting Process Simulation and Tool Wear Prediction Models," *Trans. ASME Journal of Manufacturing Science & Engineering*, Vol. 124, No. 1, 2002, pp. 42–50.

8. Sakuragi, I., et al. "Carbide Hobbing Technology for Automotive Gears," *Journal of the Japan Society for Precision Engineering*, Series C, Vol. 67, No. 655, 2001, pp. 221–226.

9. Stabler, G.V. "The Fundamental Geometry of Cutting Tool," *Proceedings of the Institution of Mechanical Engineers*, London, Vol. 165, 1951, pp. 14–26.

10. Shamoto, E. "Study on Three Dimensional Cutting Mechanism (1st Rep.)," *Journal of the Japan Society for Precision Engineering*, Vol. 59, No. 3, 2002, pp. 408–414.

Takeji Sugimoto

is an associate professor in the department of mechanical engineering at Kurume Institute of Technology in Kurume, Japan. He has more than 25 years of experience in gear manufacturing and is a member of JSME, JSPE and the Japan Society for Design Engineering.

Akira Ishibashi

is a professor and head of the graduate school in the department of mechanical engineering at Sojo University in Kumamoto, Japan. He has more than 40 years of experience in gear manufacturing. He was awarded for his research on gear grinding machines by JSME in 1970. Ishibashi is a member of JSME, JSPE, Japan ASME, Society of Tribologists, Society of Automotive Engineers of Japan and the Japanese Society of Strength and Fracture of Materials.

Masataka Yonekura

is a professor in the department of mechanical engineering at Kurume National College of Technology, a technical school established by the Japanese government. He has more than 30 years of gear manufacturing experience and is a member of JSME and JSPE.

Tell Us What You Think . . .
Visit *www.geartechnology.com* to
- Rate this article
- Request more information
- Contact the article mentioned
- Make a suggestion

Or call (847) 437-6604 to talk to one of our editors!

Klingelnberg, A/W Systems Form Alliance

Klingelnberg Oerlikon Technology Center (KOTC) of Saline, MI, joined forces with A/W Systems Co. of Royal Oak, MI, to provide spiral bevel and hypoid bevel tooling and tooling technology services.

KOTC and A/W Systems will provide cutterheads, blade sticks, finished blade grinding and gear cutting technology services to the U.S. gear manufacturing market.

According to A/W Systems' press release, the strategy is to offer locally a comprehensive product line of cutting tools with application engineering expertise and cutter sharpening services.

Mitsubishi Gear Center Partners With Balzers

The Mitsubishi Gear Technology Center of Wixom, MI, teamed up with Balzers Inc.'s Wixom Coating Center to provide local coating service for Mitsubishi brand hob cutters.

Previously, Mitsubishi's coating operations took place in its Addison, IL, machine tools facility under the name Mitsubishi SuperDry coating. After economic consideration, the company decided the Balzers BALINIT® FUTURA NANO coating was of the same quality. Also, with Balzers' nationwide coating centers, large batch runs and strict quality control, Mitsubishi found that it was not cost effective to compete with Balzers, according to Mitsubishi's newsletter.

Schafer Acquires Chicago Gear Works

Schafer Gear Works of South Bend, IN, acquired the assets of Chicago Gear Works of Cicero, IL.

Chicago Gear Works was a major supplier to industrial manufacturers and Schafer hopes this acquisition will increase its manufacturing capacity with bevel gear and worm gear technology, according to Schafer's press release.

Chicago Gear's manufacturing operations have been moved to South Bend and its turning operations to Schafer's precision machining plant in Fort Wayne, IN.

AGMA Releases New Information Sheet

The American Gear Manufacturers Association (AGMA) released an information sheet called *Accuracy Classification System—Tangential Measurement Tolerance Tables for Cylindrical Gears*.

The publication provides inch and metric tables of the tolerances dealing with tangential measurements of spur and helical gears for the different accuracy grades explained in ANSI/AGMA standard 2015-1-A01.

According to the AGMA newsletter, the sheet was developed to supplement the information contained within the standard. While the tables may be used to estimate the tolerances for an individual gear, the actual tolerances should be calculated and rounded according to the formulas of the parent standard.

New General Manager at General Broach

S. David Graham

S. David Graham was named general manager of the cutting tool division at General Broach Co. of Shelby Township, MI.

Since 1993, Graham has worked as national sales manager of General Broach. Prior to that, he held the positions of both chief tool engineer and engineering manager.

Among his new responsibilities will be developing strategic alliances with broaching partners in Europe.

Philadelphia Gear Offers Western Gear, WesTech Renewal Parts

Philadelphia Gear Corp. announced the availability of genuine renewal parts for Western Gear and WesTech gearing units.

The company acquired the brands Western Gear and WesTech in 1996 and is the only proprietary source for those parts, according to the company's press release. With these units, maintenance engineers can have their Western Gear and WesTech units serviced using genuine parts instead of re-engineered ones.

In addition, Philadelphia Gear can provide original drawings of Western Gear and WesTech gearing units. Digitally scanned versions of these drawings and bills of material will be available at the company's five regional service centers by the end of 2003.

New President, Expanding Facility for Machine Tool Systems

Jerry Rex

Jerry Rex was appointed president of Meritage Inc.'s subsidiary Machine Tool Systems (MTS) of Charlotte, NC.

According to the company's press release, Rex has 26 years' experience in metalworking and in the application of machine tools to manufacturing processes. Currently, he chairs the Machine Tool Engineer Certification Committee of the American Machine Tool Distributors' Association (AMTDA).

In other news, MTS announced plans to consolidate operations from Georgia and South Carolina into an expanded Charlotte Technical Center.

Timken Completes Torrington Acquisition

The Timken Co. of Canton, OH, announced Feb. 18 the completion of its purchase of The Torrington Co. from Ingersoll-Rand for $840 million.

Of the $840 million, $700 million was paid in cash and the remaining $140 million was in Timken shares.

According to the company's press release, this acquisition was the largest in Timken's history, increasing Timken's size by 50 percent and making it the world's third largest bearing company, with an expanded portfolio of automotive and industrial bearing-based products and services.

The Timken Co. manufactures engineered bearings, alloy and specialty steels and provides related services.

New Powder Metal Company in Pennsylvania

Vision Quality Components is a new manufacturer of particulate material structural and multilevel components for the transportation, industrial and consumer product markets. This new company is a continuation of Innex Powder Metal of Rochester, NY, whose assets were purchased in January.

The company's capabilities range from pressing between 20-200 tons, sintering, steam treating, vibratory finishing, CNC turning and double disc grinding, according to its press release.

Dennis Johns will serve as president and Robert Aleksivich as vice president of Vision, which is located in Clearfield, PA.

SMW Autoblok Partners with LNS America

SMW Autoblok, a manufacturer of power chucks located in Wheeling, IL, partnered with bar feed supplier LNS America of Cincinnati, OH. The plan is to combine SMW's steady rests with LNS's bar feed products to major turning machine OEMs and their dealer networks.

With the alliance, LNS America can provide turnkey, manual and automatic steady rest packages that include base systems and brackets, according to the company's press release.

SMW is best known for its precision workholding devices.

In Memoriam

Marlis Tetteroo, of Teco Werkzeugmaschinen GmbH & Co., a gear machinery specialist located in Hilden, Germany, died March 8 after a long illness.

Tell Us What You Think . . .
Visit *www.geartechnology.com* to
- **Rate this column**
- **Request more information**
- ***Contact the companies mentioned***
- **Make a suggestion**

Or call (847) 437-6604 to talk to one of our editors!

CLASSIFIEDS

SERVICE

Rates—Line Classified: 1" minimum, $325. Additional lines $45 per line (8 lines per inch). Display Classified: 3" minimum: **1X**—$735, **3X**—$685 per insertion, **6X**—$645 per insertion. Additional per inch: **1X**—$255, **3X**—$235 per insertion, **6X**—$225 per insertion. **Color Classified:** Add $150 per insertion for color. *Gear Technology* will set type to advertiser's layout or design a classified ad at no extra charge. **Payment:** Full payment must accompany classified ads. Send check drawn in U.S. funds on a U.S. bank or Visa/MasterCard/American Express number and expiration date to *Gear Technology*, P.O. Box 1426, Elk Grove Village, IL 60009. **Agency Commission**: No agency commission on classified ads. **Materials Deadline:** Ads must be received by the 15th of the month, two months prior to publication. **Acceptance:** Publisher reserves the right to accept or reject advertisements at his discretion.

SERVICE

WEBSITES

A Bicycle with REAL Gears

The Addendum team was in Chicago in early March, for the National Manufacturing Week show, when it saw something unusual: a bicycle with gears. Real gears. Spiral bevel gears, in fact.

The mountain bike was at Suhner Manufacturing's booth, on a small platform. The bike was on loan for the show from its maker, Christini Technologies Inc. of Philadelphia, PA.

Suhner was featuring the bike because it manufactures the bike's three spiral bevel gear sets for Christini.

Now, the Addendum team knows regular bikes don't have gears. Being gear goofs, we've known for years that regular bikes' "gears" are really sprockets.

So, why do Christini bikes have real gears?

Because they're all-wheel-drive bicycles. Power can move back and forth between the bikes' wheels via a drive system, and the gears are part of that system.

Starting with the rear wheel, the system has a spiral bevel gear (92 mm O.D., 45 teeth) and pinion (30 mm O.D., 12 teeth) that are opposite the bike's sprocket assembly. This gear set connects to a drive shaft, which itself runs through the bike's rear suspension. From there, the drive system goes inside the bike's frame, in the top tube (the horizontal bar between the seat and handlebar).

A second drive shaft runs inside the top tube to the head tube, where the handlebar is mounted. Inside the tube is the system's second spiral bevel gear set, two miter gears (34 mm O.D., 15 teeth each).

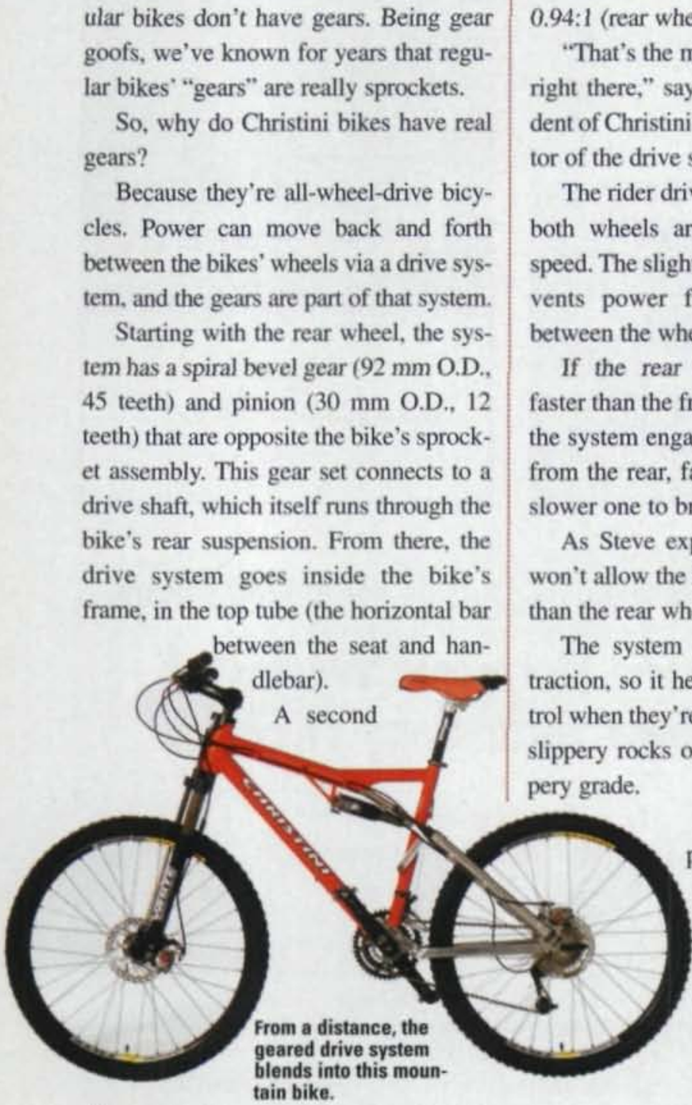

From a distance, the geared drive system blends into this mountain bike.

A third drive shaft runs down the front fork to the front wheel's hub and connects to the third spiral bevel gear set. The hub is a zero-backlash freewheel hub with a roller clutch mechanism. The gear set is a spiral bevel gear (83 mm O.D., 48 teeth) and pinion (26 mm O.D., 12 teeth). Also, these steel gear sets have a coating impregnated with Teflon® lubricant.

The bikes' overall ratio is about 0.94:1 (rear wheel to front wheel).

"That's the magic of the drive system right there," says Steve Christini, president of Christini Technologies and inventor of the drive system.

The rider drives the system so long as both wheels are rotating at the same speed. The slight gearing differential prevents power from being transferred between the wheels.

If the rear wheel slips, it'll spin faster than the front wheel. At this point, the system engages and transfers power from the rear, faster wheel to the front, slower one to bring them back in sync.

As Steve explains, the drive system won't allow the front wheel to go slower than the rear wheel.

The system transfers power to add traction, so it helps riders maintain control when they're riding over wet roots or slippery rocks or when climbing a slippery grade.

The system weighs 2 pounds 11 ounces and is engaged with the flip of a switch on the handlebar. When it isn't engaged, the bike rides like a regular mountain bike.

Look close, (with a helping hand) and you'll see this bike has a spiral bevel gear and pinion. In fact, the bike has three spiral bevel gear sets.

Steve came up with the idea for his system when he was riding his mountain bike in a park, trying to climb a muddy slope. While his rear wheel was slipping and sliding, Steve had the first, often exasperated, thought of invention—"There must be an easier, better way to do this."

That was the summer of 1994, before Steve (a mechanical engineering major, of course) graduated from Villanova University. That next school year, Steve developed his idea into a prototype for his senior design project.

In the summer of 2002, Steve's system became commercially available on his all-wheel-drive mountain bikes.

For National Manufacturing Week, Steve made one of his bikes available to Joe Agro, field sales manager for Suhner, located in Rome, GA.

Suhner's interest—and the Addendum team's interest—in featuring a Christini all-wheel-drive bike was simple.

"It was a unique application for spiral bevel gears," Joe says.

Tell Us What You Think . . .
Visit *www.geartechnology.com* to
- **Rate this column**
- **Request more information**
- **Contact the organizations mentioned**
- **Make a suggestion**

Or call (847) 437-6604 to talk to one of our editors!